Received: 31 December 2021 | Revised: 15 February 2022 | Accepted: 17 March 2022

DOI: 10.1002/cey2.219

REVIEW

CARBON ENERGY WILEY

Carbon nanomaterials and their composites for supercapacitors

Mingzhu Zhong | **Miao Zhang** | **Xifei Li**

School of Physics and Materials Science, Tianjin International Joint Research Centre of Surface Technology for Energy Storage Materials, Tianjin Normal University, Tianjin, China

Correspondence
Miao Zhang, School of Physics and Materials Science, Tianjin International Joint Research Centre of Surface Technology for Energy Storage Materials, Tianjin Normal University, 300387 Tianjin, China.
Email: miaozhang@tju.edu.cn

Funding information
National Natural Science Foundation of China, Grant/Award Number: 52102050; Science & Technology Development Fund of Tianjin Education Commission for Higher Education, Grant/Award Number: 2019KJ092

Abstract

As a type of energy storage device between traditional capacitors and batteries, the supercapacitor has the advantages of energy saving and environmental protection, high power density, fast charging and discharging speed, long cycle life, and so forth. One of the key factors affecting the performance of supercapacitor is the electrode material. Carbon materials, such as carbon nanotube, graphene, activated carbon, and carbon nanocage, are most widely concerned in the application of supercapacitors. The synergistic effect of composites can often obtain excellent results, which is one of the common strategies to increase the electrochemical performance of supercapacitors. To further improve the performance of binary composites, it is a relatively simple method to increase the components as the "bridge" between the two materials to form the ternary composites. The review mainly introduces the current research progress of supercapacitors with pure carbon nanomaterials and multistage carbon nanostructures (composites) as electrodes. The characteristics and application directions of different pure carbon nanomaterials are introduced in detail. Different ways of multilevel structure (material) composite have their own effects on the development of high-performance supercapacitors. We also highlight the recent advances related to these fields and provide our insight into high-energy supercapacitors.

KEYWORDS
binary composite, carbon nanomaterials, supercapacitors, ternary composite

1 | INTRODUCTION

In recent years, with the rise of aerospace, renewable energy, electric vehicles, and intelligent electronic equipment, as well as the increasing energy shortage and environmental crisis, the development of clean, efficient, and sustainable energy has become increasingly important. The development of energy storage equipment has achieved more and more attention. As a new type of high-efficiency energy storage device, the supercapacitor has a higher energy density than a traditional capacitor higher power density and longer cycle life compared with a secondary battery.[1] It is a potential energy storage device between a traditional capacitor and battery. In the production process, researchers can avoid heavy metals and other harmful chemicals and select appropriate precursors, such as biomass,[2] to reduce environmental pollution. Compared with other conventional capacitors, supercapacitors are less

This is an open access article under the terms of the Creative Commons Attribution License, which permits use, distribution and reproduction in any medium, provided the original work is properly cited.
© 2022 The Authors. *Carbon Energy* published by Wenzhou University and John Wiley & Sons Australia, Ltd.

polluting and are often referred to as "green energy." Supercapacitors originated from Helmholz's theory of electric double layer in 1879. Then in 1957, Becker applied for the first patent of the electrochemical capacitor based on the activated carbon (AC) with a high specific surface area as electrode material.[3] Five years later, Standard Oil (SOHIO) produced a 6 V supercapacitor using AC as the electrode material and sulfuric acid (H_2SO_4) solution as the electrolyte. For the first time, the company commercialized the electrochemical capacitor with carbon electrode material in 1969. At present, supercapacitors are widely used in military equipment,[4] aerospace,[5,6] rail transit,[7] new energy vehicles,[8,9] power generation system,[10,11] intelligent electronic equipment,[12] and other fields. As a kind of energy storage device with high power density, fast charge–discharge speed, and long cycle life, supercapacitors also have some problems, such as high self-discharge rate, low specific capacitance, and low energy density. According to different working modes, supercapacitors can be divided into electric double-layer supercapacitors and pseudocapacitor supercapacitors. Electric double-layer supercapacitors rely on the electric double layer between electrolyte/electrode to store and transfer charge. In addition to the electric double-layer energy storage mode, the pseudocapacitor supercapacitor also has the redox energy storage mode based on the rapid redox reaction between electrolyte and electrode materials. In electric double-layer supercapacitor devices, the anode and cathode are electrically isolated by an ion-permeable membrane.[13,14] As shown in Figure 1A, the external electric field causes the positive and negative ions in the electrolyte to be aligned on the negative/positive solid–liquid interface of the capacitor, respectively. During charging, the excess charge accumulates on the positive and negative plate surface of the capacitor, and the ions with opposite charge in the electrolyte will be aligned on the positive and negative solid-liquid interface to form an electric double layer. During discharge, the positive and negative plates transfer charge through the conductive external circuit, the amount of excess charge is reduced, and the opposite charge at the corresponding solid-liquid interface returns to the electrolyte, so as to realize the storage and release of energy.[1] As shown in Figure 1B, in the pseudocapacitor supercapacitor, ions are adsorbed on the positive and negative plates and undergo a redox reaction with surrounding substances to realize energy storage.[15,16] This redox reaction is a variable potential reaction without voltage platform and has capacitance characteristics, which is called pseudo capacitance reaction. Therefore, the electrode material is the most critical part of the supercapacitor and the basis of energy storage of the supercapacitor.

Carbon nanomaterials, such as carbon nanotubes (CNTs), graphene (GR), AC, and carbon nanocages (CNCs), are the most widely studied and applied electrode materials for supercapacitors.[1,3] They have their own advantages. CNTs with one-dimensional (1D) structure have relatively regular pore structure, large specific surface area, high conductivity, and chemical stability.[17] GR with a 2D structure has a large specific surface area, high electrical conductivity, and stable thermal and chemical properties.[18] AC has the advantages of low cost, simple synthesis process, good conductivity, large specific surface area, and stable electrochemical performance.[19] CNCs with a 3D structure have the advantages of a multiscale pore network, large specific surface area, uniform pore size distribution, good conductivity, and so on.[20] At the same time, on the basis of single carbon nanomaterials, it is an important research direction to optimize and composite them to meet the performance requirements of supercapacitors.

Here, we review the latest research progress of supercapacitors with pure carbon nanomaterials and multilevel carbon nanostructures (composites) as electrodes. In addition, the characteristics and application directions of different pure carbon nano materials and multilevel structure (material) composites are emphatically introduced

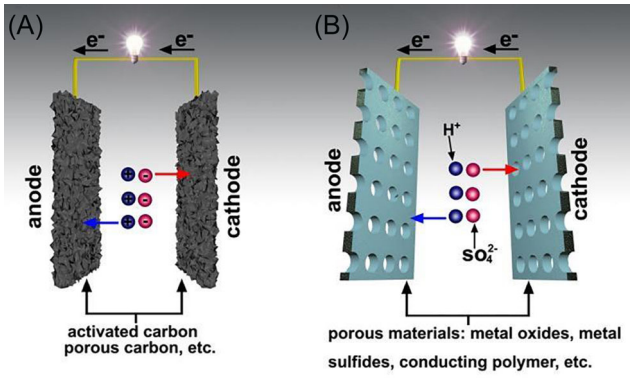


FIGURE 1 Schematic diagram of (A) an electrical double-layer capacitor and (B) a pseudocapacitor. Reproduced with permission: 2016, The Royal Society of Chemistry.[15]

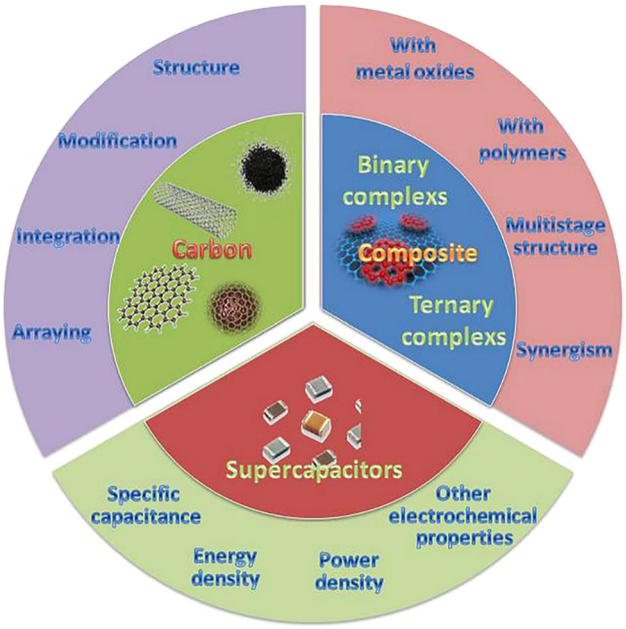


FIGURE 2 Structure overview of this article.

(Figure 2). Different composite methods of multilayer structures (materials) have their own effects on the development of high-performance supercapacitors of multilevel structure (material) composite have their own effects on the development of high-performance supercapacitors. Finally, the application and development direction of carbon nanomaterials in supercapacitors are prospected, which provides some guidance for the research of carbon nanomaterials for supercapacitors.

2 | CARBON NANOMATERIALS

Many kinds of carbon nanomaterials are highly researched to obtain improved capacitance, such as AC, CNTs, GR, CNCs, and many others. Their natural abundance in different forms and low cost make them an ideal candidate for supercapacitor applications. In addition, surface area and conductivity can easily be tuned in the carbon. At present, extensive research is being performed using various carbon materials, and the main objective is to improve the performance of carbon-based supercapacitors.

2.1 | 1D carbon material

2.1.1 | CNTs

CNTs are a kind of nanosized tubular carbon materials discovered in the early 1990s. They are seamless hollow tubes made of single or multilayer GR sheets. CNTs are typical 1D carbon nanomaterials, which have the advantages of regular pore structure, large specific surface area, high conductivity, and chemical stability; they have potential application value in the field of supercapacitor. Due to their unique hollow structure, good conductivity, large specific surface area, suitable pores for electrolyte ion migration (pore diameter generally > 2 nm), and the formation of nanoscale network structure by cross winding, they are considered to be an ideal electrode material for supercapacitors, especially for high-power supercapacitors. CNTs exhibit comparable capacitance values to AC, although AC possesses a larger surface area. The great performance of using CNTs is ascribed to the utilization of the maximum surface area of CNTs for continuous charge distribution. Furthermore, their mesoporous characteristics allow electrolytes to diffuse more easily to reduce the equivalent series resistance and thus improve the power output. In recent years, it has attracted extensive attention and become one of the research hotspots. Related studies explored the preparation process, normalization, and array of CNTs to obtain CNTs electrode materials with excellent electrochemical properties.

Hussain et al.[21] prepared the vertically aligned multiwalled carbon nanotubes (VA MWCNTs) by plasma-enhanced chemical vapor deposition (CVD). A simple and rapid nitrogen plasma treatment was used to remove the amorphous carbon and introduce nitrogen-containing functional groups into the edge and base surface of MWCNTs without destroying their vertical arrangement. In an aqueous solution, the specific capacitance of the treated nanotubes increases from 22 to 55 F/g at a scanning rate of 10 mV/s after treatment with 75 W and 260 Pa nitrogen plasma. Shi and Zhitomirsky[22] prepared uniformly coated MWCNTs by using persulfate $(CTA)_2S_2O_8$ as a dispersant of MWCNTs and oxidant of PPy polymerization. Among them, Ponceau S (PS) dye is a new anion dopant. The uniformly coated MWCNTs have a high specific capacitance (4.1 F/cm^3 at a scanning rate of 2 mV/s) and good cyclic stability (capacitance retention rate of 94.4% after 1000 cycles). For the first time, Yang et al.[23] synthesized CNTs in situ using a novel metal organic framework (MOF) precursor as raw material (MOF precursor as the only carbon source, catalyst, and reducing agent). The electrode materials obtained from the CNTs have high specific capacitance (272 and 168 mF/cm^2 at 0.5 and 10 mA/cm^2, respectively), high energy density (0.0544 mWh/cm^2), high power density (5.988 mW/cm^2) and excellent cycle stability (even after 5000 charge–discharge cycles, 100% high retention value can be obtained). Cao et al.[24] used thermal annealing in an atmospheric environment and developed a new type of highly scalable and reliable supercapacitor by transferring CNTs that are bent vertically arranged to elastomer substrate. The fabrication process of crumpled-CNT forest electrodes and the

morphology of CNTs are shown in Figure 3A–D. Due to the flexibility and intertwined networks formed in the crumpled CNT forests, the shrunk CNTs forest electrode exhibits excellent electrochemical performance under large uniaxial or biaxial strain. The bent CNTs forest electrodes exhibited good electrochemical performance and stability under uniaxial (300%) and biaxial (300% × 300%) strain after thousands of tensile relaxation cycles (the retention rate was 85% after 10,000 constant-current charge–discharge cycles were observed under 1 mA/cm^2). Figure 3E–M is an electrochemical performance diagram of uniaxial stretchable all-solid-state supercapacitors using collapsed CNTs as electrodes, and polymer gels as electrolytes and diaphragms. At a scanning rate of 50 mV/s, the obtained supercapacitor can maintain a tensile capacity of 800%, with a specific capacitance of 5 mF/cm^2. Adusei et al.[25] modified the surface of CNT fibers by atmospheric pressure plasma functionalization, which significantly improved the electrochemical properties of CNTs. The plasma functionalization method improves the specific surface area of CNT fibers (the surface area of CNT fibers increases from 168.22 to 208.01 m^2/g) and specific capacitance. In addition, the fiber supercapacitor assembled from this material shows good cycle stability (the capacitance remains 93.2% after 4000 cycles).

Free-growing CNTs have disordered orientations and different morphologies. Meanwhile, they are either clustered into bundles or intertwined with each other, so it is difficult to purify them. In recent years, the ordered and arrayed CNTs have attracted much attention.

Fedorovskaya et al.[26] used aerosol-assisted catalytic CVD technology to fabricate the vertically oriented CNTs on an N-doped silicon substrate and studied their supercapacitor behaviors. The results show that when the array thickness is between 200 and 800 μm, the aligned CNTS have a larger specific capacitance than the disordered nanotubes (the maximum specific capacitance of the ~280 μm array is 124 F/g at a scanning rate of 20 mV/s). Childress et al.[27] used lignin as an electroactive polymer to investigate the electrochemical properties of helical carbon nanotubes (HCNTs) at two electrodes (as vertically aligned arrays [VHCNTs] and as freestanding polymer-augmented HCNT buckypapers [HCNT BPs]). The results showed that the specific capacitance of HCNT and MWCNT BPs were 593 mF/cm^2 (125.0 F/g) and 379 mF/cm^2 (69.7 F/g), respectively. At the same time, HCNT BPs exhibited a capacity superior to MWCNT BPs as it adsorbed more sodium lignosulfate.

CNTs have been used directly as electrode materials for supercapacitors, which is of great significance for the application of CNTs in supercapacitors. In general, the research focuses on the following aspects: preparation of CNTs with high specific surface area and high purity to obtain high specific capacity; improving pseudocapacitance by producing abundant surface functional groups while increasing the infiltration with the electrolyte; reducing internal resistance and improving power characteristics by optimizing the electrode manufacturing process, or by directly growing carbon nanotubes on a conductive substrate to prepare integrated electrodes, or by structure and array of carbon nanotubes.

2.2 | 2D carbon material

2.2.1 | GR

GR is a kind of hexagonal 2D carbon nanomaterial with a honeycomb lattice composed of carbon atoms with an sp^2 hybrid orbital. It has many advantages, such as large theoretical specific surface area, high electrical conductivity, stable thermal and chemical properties, and so forth. As the electrode material, GR is expected to improve the overall performance of supercapacitors. Due to these outstanding features, these materials have been exploited in different forms for energy storage devices. However, extraordinary characteristics of GR showed specific capacitances in various electrolytes (aqueous [135 F/g], organic [99 F/g], and ionic liquid [75 F/g] electrolyte), which are much lower than the expected theoretical capacitance value due to a decreased double layer formation. Therefore, it has been suggested that the theoretical capacitance value can only be attained when all active sites of the GR electrode surface are accessible to electrolytes.

Li et al.[28] used surfactant (Tween-20) as a carbon source (molecular precursor) and adopted the simple and effective buried protection KOH activation technology to prepare a novel 3D GR-like carbon nanosheets network. Due to the excellent 3D network structure and layered porous structure, the 3D GR-like carbon nanosheets have a large specific surface area (2017.3 m^2/g), high specific capacitance (316.8 F/g), and good cycle stability (the retention rate is 92.5% after 2000 cycles). Lu et al.[29] prepared GR with high surface area (1057 m^2/g), high specific capacitance (251 F/g), and good cycle stability (capacity retention rate of 96.4% after 1000 cycles) by simple activation hydrothermal method using biomass precursor (Australian nutshell) as raw material. The GR-like carbons have the perfect GR-like structure and abundant micropores and mesopores. These results indicate that GR-like structure has good electrochemical performance and has a certain application prospect in the field of supercapacitors. He et al.[30] proposed a simple and low-cost top-down method to prepare porous GR fibrous structure and applied it to the micro supercapacitors with outstanding performance. The prepared porous GR fibers exhibited good electrochemical properties when assembled

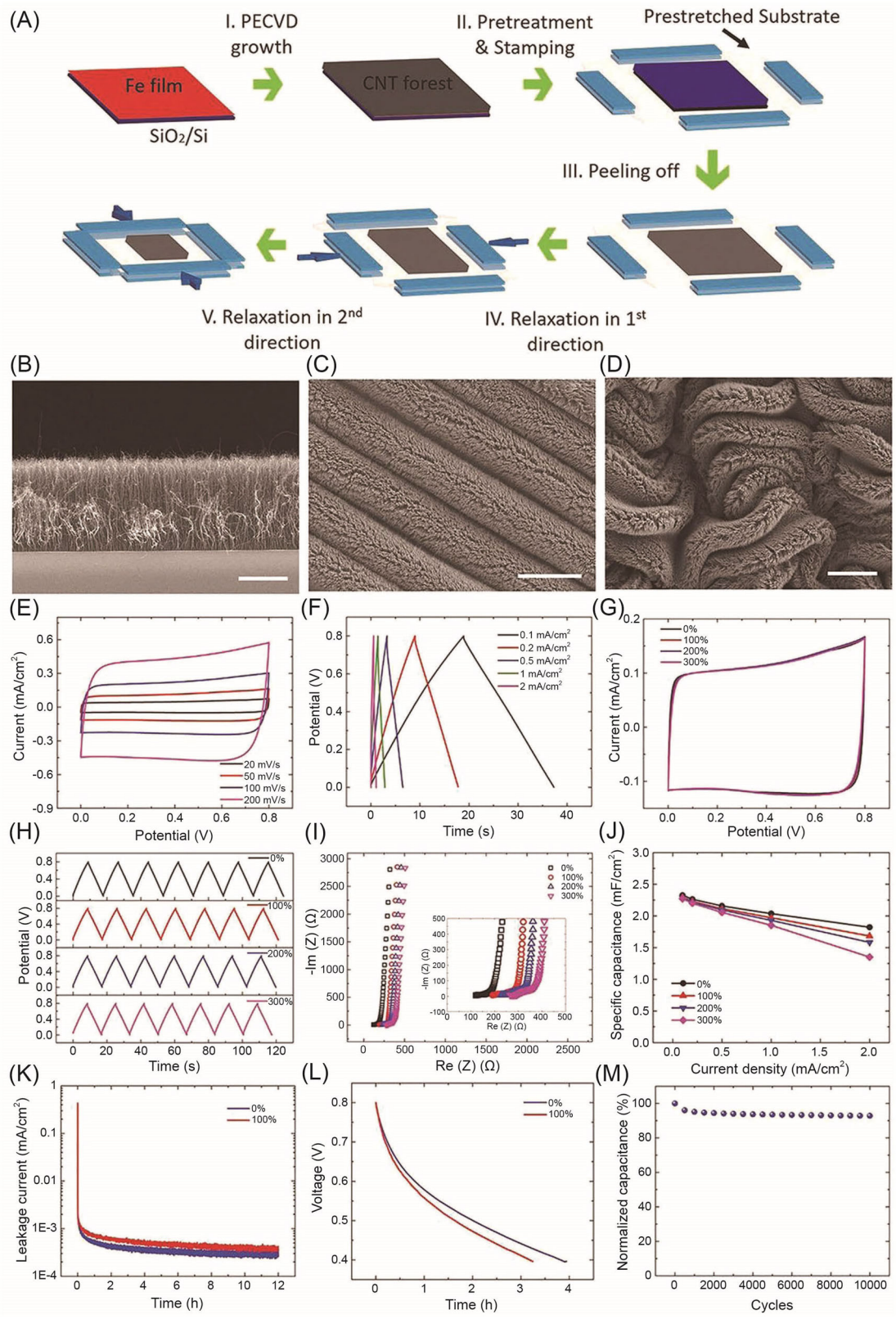


FIGURE 3 (See caption on next page)

into micro supercapacitors (high electrochemical capacitance of ~247.6 mF/cm^2 at ~2 mA/cm^2 and low equivalent series resistance of ~2.4 Ω) and all solid state flexible micro supercapacitors (H_3PO_4/PVA has a high area capacitance of 70.6 mF/cm^2 and a good cycle stability of ~96% capacitance after 2400 cycles). It shows that the porous GR fiber electrode has a good application prospect in the field of microelectronic equipment and flexible energy storage.

GR is a good candidate for electrode material of supercapacitors. However, owing to the strong van der Waals and π-π interaction force between GR sheets, GR sheets are often stacked together, which can significantly reduce the specific surface area utilization. To solve the stacking problem, some researchers modify GR to enhance the conductivity for the application of supercapacitors.[31] Yuan et al.[32] proposed a strategy for the design and fabrication of nanostructures based on porous graphene skeleton (PGFs). Figure 4A is a synthesis strategy diagram for generating PGFs, in which in-situ covalent functionalization of RGO with 4-iodobenzene and subsequent aryl-aryl-coupling reaction were conducted. Figure 5A shows the emergence of multilayer stacking in PGFs. In the repeated charge–discharge cycle, the GR layer can improve the charge transferability of the electrode and stabilize the electrode. PGF-based supercapacitors have high energy density (maximum energy density is 6.4 Wh/kg at a current density of 0.2 A/g), high power density (maximum power density is 4560 W/kg), quite promising cycle stability (≈98% of the capacitance remains at 2 A/g after 2000 cycles), and rate capability (capacitance retention rate of 97% at a high current density of 10 A/g and 5000 cycles). Bhattacharya et al.[35] made a laser-induced GR supercapacitor. At the specific current density of 0.1 mA/cm^2, the maximum capacitance of 203 mF/cm^2 is obtained, while at the extremely high specific current density of 1 mA/cm^2, a stable capacitance of 15 mF/cm^2 is obtained. When the power density is 0.14 mW/cm^2 (compared to the current density of 0.1 mA/cm^2), the highest energy density is 51 Wh/cm^2; when the extremely high power density is 1.36 mW/cm^2 (the current density of 1 mA/cm^2), the energy density is maintained at 2 Wh/cm^2, indicating that the electrodes have great stability under high current density. The prepared electrode flexible device, in an interleave plane design, with inkjet-printed silver current collectors, has a high energy

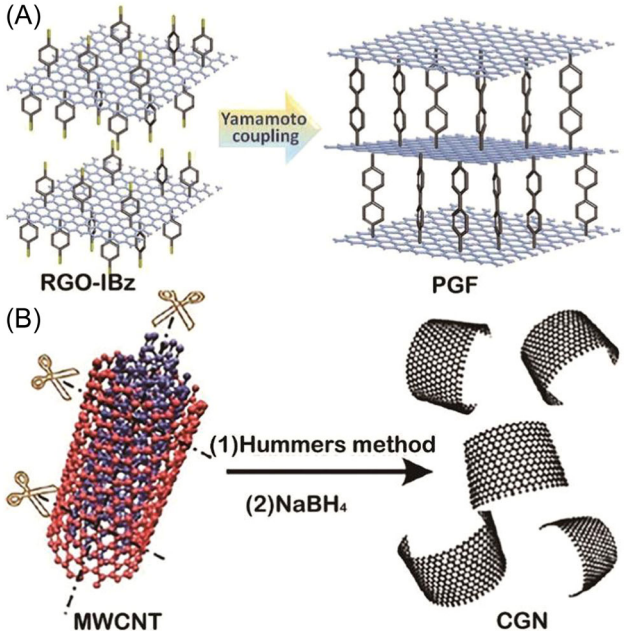


FIGURE 4 Schematic diagram of graphene synthesized by different methods. (A) Synthesis strategy for the generation of PGF. Reproduced with permission: 2015, WILEY-VCH Verlag GmbH & Co. KGaA.[32] (B) The preparation of the CGN material by combining the Hummers method and subsequent reduction with $NaBH_4$. Reproduced with permission: 2012, American Chemical Society.[33] CGN, curved graphene nanosheet.

FIGURE 3 Fabrication of crumpled-CNT forest electrodes and performance of a uniaxially stretchable all-solid-state supercapacitor with crumpled-CNT-forest as electrodes and polymer gel as electrolyte and separator. (A) Schematic fabrication process flow for stretchable supercapacitor electrodes from PECVD grown multiwall CNT forest. (B) SEM image of CNT-forest grown on a silicon wafer by PECVD for 5 min. The average height of the CNTs is around 20 μm. (C) SEM image of the parallel ridge pattern formed by the CNT-forest on an elastomer substrate after relaxation in one direction. (D) SEM image of the crumpled pattern formed by the CNT-forest on a fully relaxed elastomer substrate (300% × 300%). (E) CV curves of the supercapacitor measured at different scan rates without strain. (F) Charge/discharge curves at different current densities without strain. (G) CV curves of the supercapacitors measured at a scan rate of 50 mV/s under the different applied strains. (H) Charge/discharge curves at a current density of 0.2 mA/cm^2 under uniaxial strains from 0% to 300%. (I) Nyquist impedance plot of the stretchable supercapacitor at different strains from 0% to 300%. (J) Specific capacitance of the supercapacitors measured at different current densities and under different strains. (K) Leakage current measurement of a representative supercapacitor with and without 100% strain. A DC voltage of 0.8 V was applied across the capacitor; the current required to retain that voltage was measured over a period of 12 h. (L) Self-discharge curves of the same representative supercapacitor with and without 100% strain, obtained immediately after precharging to the maximum voltage of 0.8 V. The open-circuit voltages across the supercapacitor are recorded over 50% the operation voltage of 0.8 V versus time. (M) The normalized capacitance retention measured by charge/discharge of the supercapacitor for 10,000 cycles at 1 mA/cm^2. The solid-state electrolyte is PVA/KCl. Reproduced with permission: 2019, WILEY-VCH Verlag GmbH & Co. KGaA.[24] CNT, carbon nanotube; PECVD, plasma-enhanced chemical vapor deposition; SEM, scanning electron microscopy.

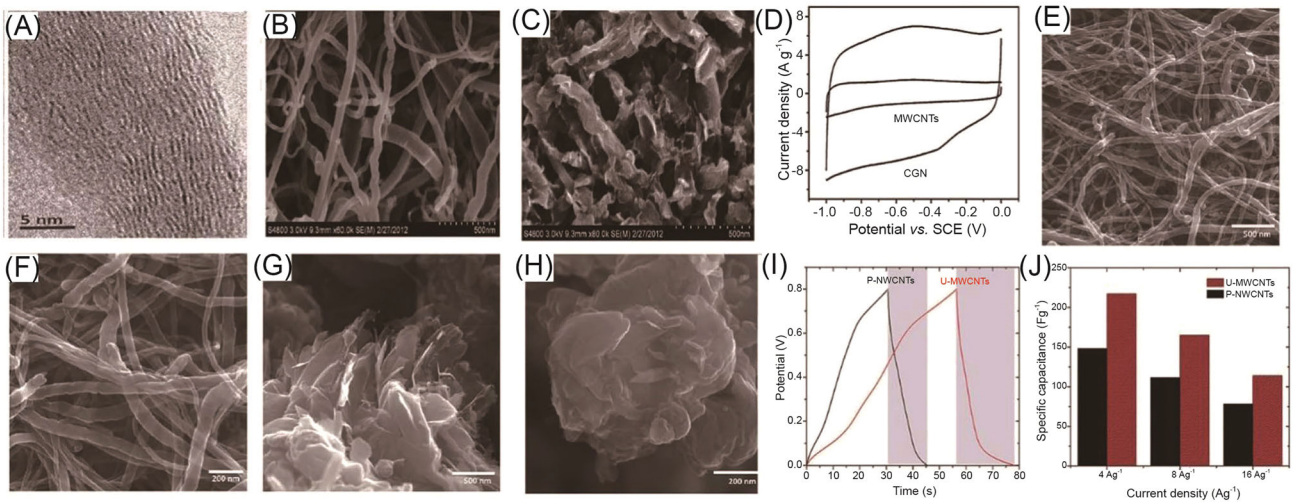


FIGURE 5 (A) HRTEM image of PGF. Reproduced with permission: 2015, WILEY-VCH Verlag GmbH & Co. KGaA.[32] FESEM images of the (B) MWCNTs and (C) CGN. (D) CV curves of MWCNTs and CGN at 50 mV/s in 6 M KOH. Reproduced with permission: 2012, American Chemical Society.[33] SEM micrographs of (E,F) MWCNTs vertically aligned (P-MWCNTs) and (G,H) unzipped MWCNTs (U-MWCNTs). (I) Galvanostatic charge/discharge curves at a current density of 4 A/g for P-MWCNTs and U-MWCNTs. (J) Plot of specific capacitance versus current density for P-MWCNTs and U-MWCNTs. Reproduced with permission: 2018, Elsevier B.V.[34] CGN, curved graphene nanosheet; FESEM, field emission scanning electron microscopy; HRTEM, high-resolution transmission electron microscopy; MWCNT, multiwalled carbon nanotube; SEM, scanning electron microscopy.

density of 0.018 mWh/cm^2 at 0.66 mW/cm^2 power density. The capacitance maintains 81% after 4000 cycles. It also has good bending resistance and bending performance.

In addition to the modification of GR, the decompression and cutting of CNTs also can be used to form GR sheets, which combine the advantages of 1D CNTs and 2D GR, hinder the accumulation of GR, and improve their electrochemical performance. Wang et al.[33] directly cut and decompressed multiwalled carbon nanotubes (MWCNTs) by the Hummers' method and reduced the conjugated network by $NaBH_4$, forming curved graphene nanosheets (CGNs) for the application in supercapacitors. Figure 4B is a diagram for preparing CGN material. The preparation process includes two steps, oxidation using the Hummers method and reduction with $NaBH_4$. Figure 5B shows the commercially produced MWCNTs. It can be seen that these MWCNTs are curved and entangled, with diameters ranging from 40 to 100 nm and lengths in the range of microns. From Figure 5C, it can be found that these shorter CNTs have been decompressed longitudinally, and a tubular GR sheet structure can be found. Figure 5D is CV curves of MWCNTs and CGN at 50 mV/s in 6 M KOH. The research shows that the specific capacitance of CGNs can reach 256 F/g when the current density is 0.3 A/g in 1 M KOH solution. At a current density of 10 A/g, the capacitance is more than 71% compared with 0.3 A/g in 1 M Na_2SO_4. A constant current charging–discharge cycle was used to carry out a durability test at 5 A/g, and the results show that CGN have good cycling stability. In 1 M KOH, the CGN electrode can maintain 99% of its initial value over 5000 cycles. In 1 M H_2SO_4, the specific capacitance of the sample increases with the number of cycles. In 1 M Na_2SO_4, the attenuation of specific capacitance is only 3% after 5000 cycles. Silva et al.[34] reported a simple method to decompress CNTs to produce GR sheets with high crystalline quality. Structural and morphological modifications of the unzipping process were investigated using the scanning electron microscopy (SEM) technique. The SEM micrographs of MWCNTs vertically aligned (P-MWCNTs) and unzipped MWCNTs (U-MWCNTs) are shown in Figure 5E–H. The improvement of CNT capacitance can be observed in the charge–discharge curve of Figure 5I. Even at high current density, the U-MWCNTs showed higher specific capacitance (the maximum specific capacitance of U-MWCNTs at 4 A/g was 217.1 F/g, while the maximum specific capacitance of P-MWCNTs was 148.1 F/g), as showed in Figure 5J. Under the current density of 4 A/g, the specific energy of U-MWCNTs was 4.8 Wh/kg, while under the same current density, the specific energy of P-MWCNTs was 3.3 Wh/kg.

To further improve the performance of GR supercapacitors, 3D GR with high specific surface areas attract more and more attention. 3D GR has rapid electron and ion transport due to the channels in porous structures and can be supported by themselves, which means that it

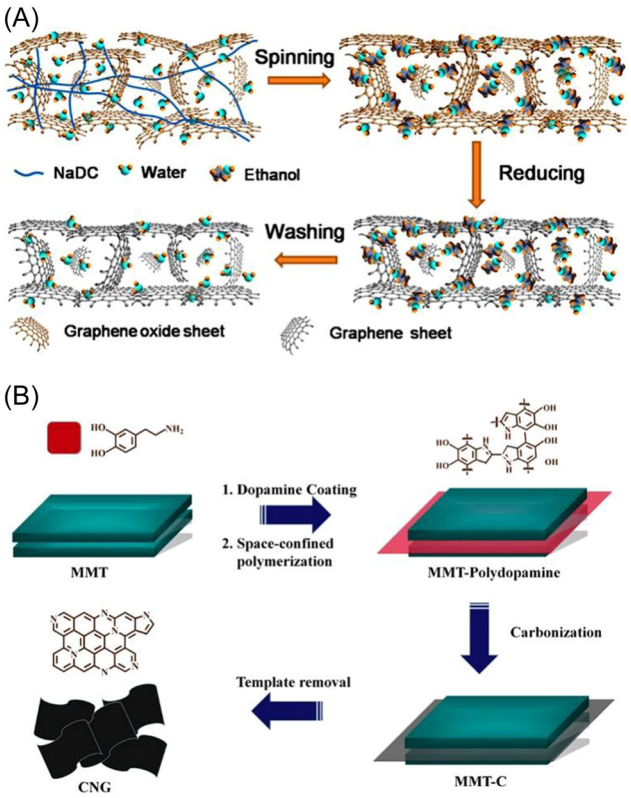


FIGURE 6 Characterization of the 3D-ts-graphene network. (A) Schematic showing the formation mechanism of the 3D graphene. Reproduced with permission: 2014, Elsevier Ltd.[37] (B) Schematic illustration of CNG synthesized through confined-carbonization strategy. Reproduced with permission: 2015, American Chemical Society.[38] 3D, three-dimensional; 3D-ts-graphene, 3D turbine graphene.

can directly serve as supercapacitor electrode material without adding binder.

Strauss et al.[36] used a combination of pyrolysis and infrared laser treatment to convert carbon nanodots into porous 3D turbine GR(3D-ts-graphene). The 3D-ts-graphene has good electrochemical performance and micropore structure which is shown in Figure 7A,B. When the current density is 560 A/L, the almost ideal capacitance behavior of 27.5 mF/L is realized. The energy density corresponding to the power density of 711 W/L is 24.1 mWh/L. After 20,000 cycles under ambient conditions, the electrode retains 94.6% of its capacitance. It is worth noting that the charge–discharge cycle rate is extremely fast, and the time constant is 3.44 ms. Huang et al.[37] fabricated 3D GR by a simple freeze-drying technique. Figure 6A shows the formation mechanism of PGRs. It is can be seen from the SEM image presented in Figure 7C–F that some wrinkles and pores can be seen on the surface, which is beneficial to providing an easy path for the electrolyte ions and achieving the excellent electrochemical performance. The supercapacitor based on the 3D GR with flexibility has a high specific capacitance of 208.7 F/g (78.3 mF/cm^2 or 3.12 mF/cm^2) and high cycling stability (99% capacitance retention after 5000 cycles). Wang et al.[38] fabricated 3D GR by blending dopamine with aqueous montmorillonite (MMT), followed by carbonizing, as illustrated in Figure 6B. The highly conductive networks, fast ion diffusion paths, and high ion-available surface area are beneficial for the application in supercapacitors. It displays outstanding gravimetric and volumetric capacitances of 128 F/g and 98 F/cm^3, respectively, as well as high gravimetric and volumetric energy densities of 56 Wh/kg and 43 Wh/L, respectively.

2.3 | 3D carbon material

2.3.1 | AC

Up until now, ACs have been widely used in the commercial applications of supercapacitors due to their excellent electrical, chemical, and thermal properties, large specific surface areas (1000–3000 m^2/g), and relatively high capacitances. However, owing to their long diffusion distance and high ion-transfer resistance, ACs have a large I_R drop and a small ion-accessible-specific surface area at high current densities, which leads to the dramatical decrease of ACs specific capacitance with an increase in the charging–discharging rate. Therefore, a large number of studies have been carried out to improve the preparation and structure of AC materials to optimize their electrochemical performance at high current densities.

2.3.1.1 | *The selection and porcessing of carbon source materials of AC for achieving excellent specific surface area and pore structure*

Chao et al.[39] used filter paper as a precursor to prepare regular and graded porous carbon electrode materials for assembling high-performance supercapacitors through simple carbonization and activation process at a relatively low temperature of 650°C (the prepared electrode material is called PFPC). The PFPC supercapacitor exhibits a high specific capacitance of 219.6 F/g and 173.0 F/g at 1 A/g and 50 A/g, respectively, indicating an excellent rate capability of 78.8%. In addition, the capacitance retention of the PFPC supercapacitor reaches 99.0% after 10,000 charge–discharge cycles at 5 A/g, demonstrating excellent cycling stability. Le Van et al.[40] prepared the AC with porous structure, various surface functional groups, and high specific surface area (S_{BET} = 2482–2681 m^2/g) from rice husk, in which the micropores and mesopores were mainly distributed between 0.9 and 3.0 nm. The results show that the specific capacitance of the electrode reaches 172.3 F/g using cyclic

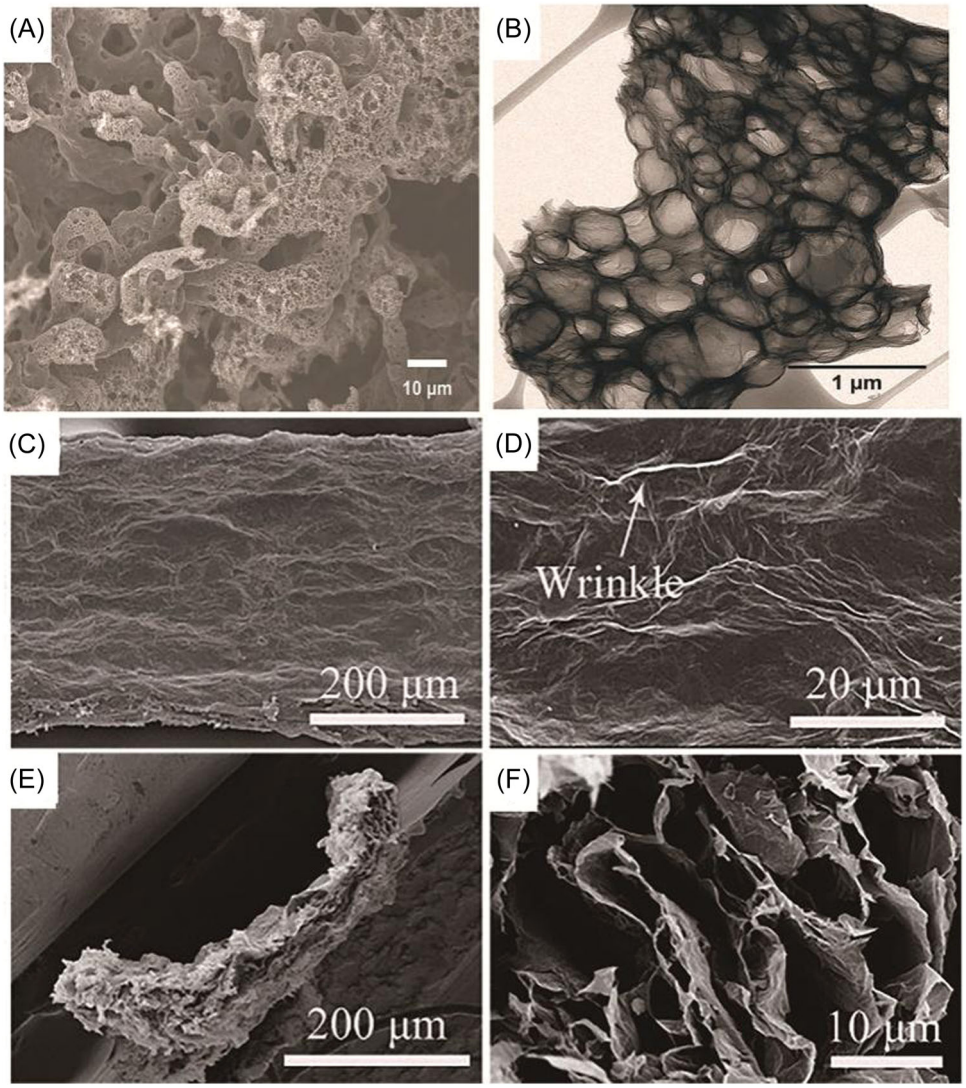


FIGURE 7 Characterization of the 3D-ts-graphene networks: (A) SEM image of 3D-ts-graphene obtained at 3 kV and (B) TEM image of a fragment of 3D-ts-graphene obtained at 120 kV. Reproduced with permission: 2018, WILEY-VCH Verlag GmbH & Co. KGaA.[36] (C–F) FESEM images of the 3D graphene. Wrinkles and pores can be seen on (C,D) the surface and (E,F) the cross section of the 3D graphene. Reproduced with permission: 2014, Elsevier Ltd.[37] 3D-ts-graphene, 3D turbine graphene; FESEM, field emission scanning electron microscopy; TEM, transmission electron microscopy; SEM, scanning electron microscopy.

voltammetry at a scan rate of 5 mV/s and 198.4 F/g at current density 1000 mA/g in the charge/discharge mode. After 1000 charge–discharge cycles, the specific capacitance is almost unchanged. Li et al.[41] prepared the AC as the electrode materials in supercapacitors with special pore structure, high specific area, specific capacitance of 207.5 F/g under the condition of the current density of 500 mA/g, and good cycling stability (89.1% after 3000 cycles) using lignite as raw material and $ZnCl_2$ as excitator. Due to the activation of $ZnCl_2$, AC has a special pore structure and high specific surface area, which improves the electrochemical performance of supercapacitors to a certain extent. Zhu et al.[42] prepared three kinds of AC (KOH-activated GC [KGC], $ZnCl_2$-activated GC [ZnGC], and H_3BO_3-activated GC [BGC]) from dead ginkgo leaves. The results show that KGC has the best specific capacitance (0.5 A/g at 374 F/g) compared with GC, ZnGC, and BGC. At the same time, the maximum energy density of KGC in the two-electrode structure can reach 9.2 Wh/g at an average power of 48 W/g. In addition, KGC materials also have good cycle performance (the initial capacitance is maintained at about 70% and 65% in 2000 and 5000 cycles), and good chemical stability (the Kentucky Coulombic efficiency in the double electrode structure is maintained at about 99% after the initial cycle). Jiang et al.[43] used hybrid willow as the raw material of lignocellulosic biomass to successfully prepare high-porosity AC with superior microporous structure and studied the electrochemical

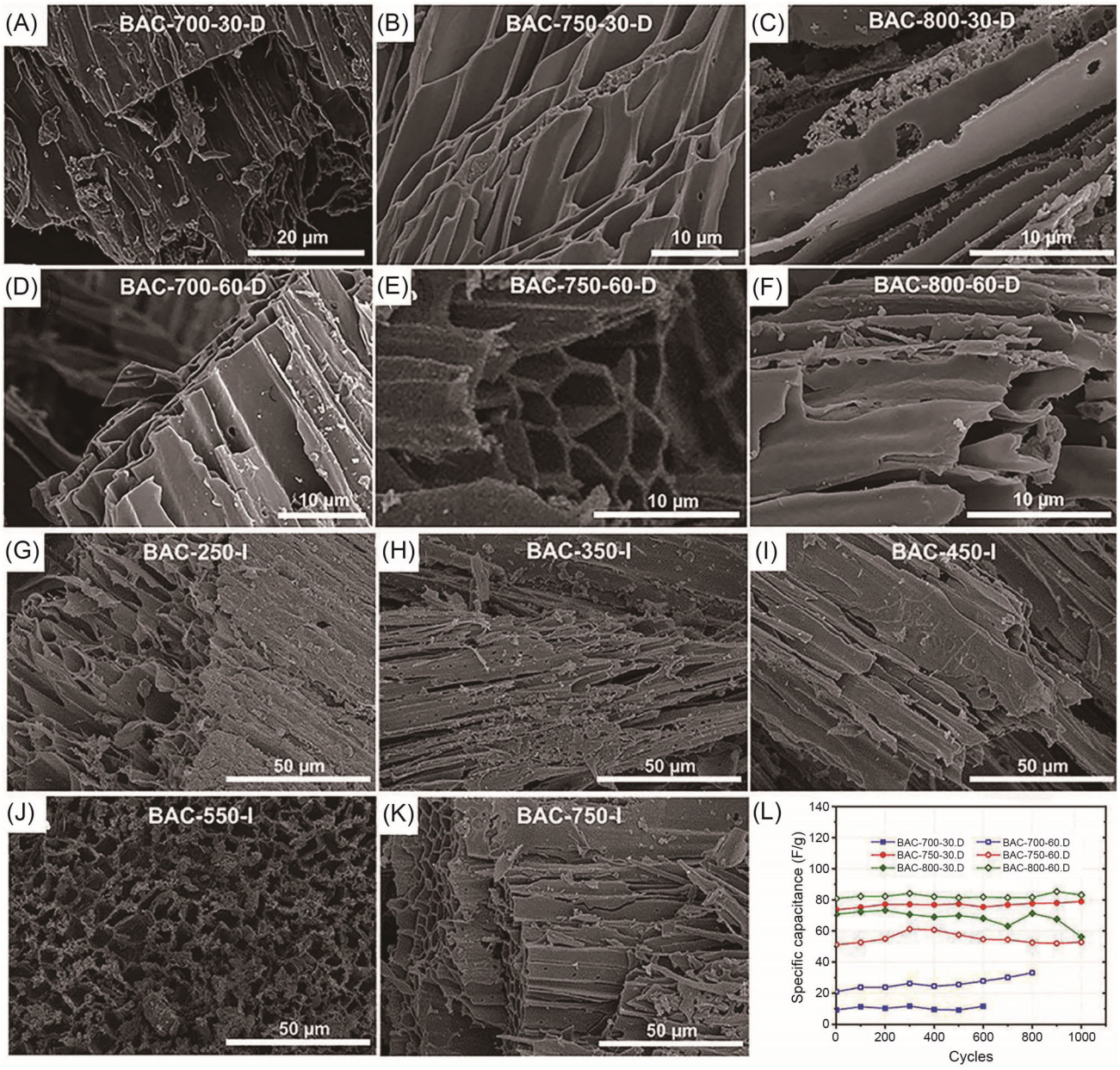


FIGURE 8 (A–F) SEM microstructures of the activated carbons prepared via direct activation route. (G–K) SEM microstructures of the activated carbons prepared via indirect activation route. (L) specific capacitances of the activated carbons as a function of cycle number (cycling stability) over 1000 cycles at 100 mA/g constant current density. Reproduced with permission: 2020, Elsevier Ltd.[43] SEM, scanning electron microscopy.

properties of two types of ACs prepared by direct and indirect CO_2 activations. The direct activation process refers to the one-step conversion of the biomass into AC using carbon dioxide (CO_2) as the activating agent. In the indirect activation route, the biomass-derived char (biochar) was first subjected to low-temperature pyrolysis, similarly followed by the physical activation using CO_2. Figure 8A–K shows the SEM images of microstructures of the ACs prepared via direct activation route and via indirect activation route, showing the developed channels that facilitate ion storage and transport. The results show that the indirect-CO_2-activation samples with higher O type I functional groups (quinone-type carbonyl) have higher capacitance (the specific capacitances of ACs by direct and indirect activation routes are 80.9 and 92.7 F/g, respectively, under the condition of constant current density is 100 mA/g) and better cycling performance (the capacitance loss is also measured as very low (<0.5%) after 1000 charge and discharge cycles, which is showed in Figure 8L), which is caused by indirect-CO_2-activation BAC samples with higher O type I functional groups (quinone-type carbonyl). Agus et al.[44] adopted the following three steps to produce

pineapple leaves (SDN): chemical activation by highly active preparations, carbonization at 600°C under the gas N_2 environment, and the physical activation at 850°C for 2 h under the CO_2 gas. The specific surface area of the electrodes produced was 512.211 m^2/g, the total pore volume was 0.093 cm^3/g, and the average pore radius was 1.199 nm. The diameter of the fiber is 101–185 nm. The fiber diameter on the activated carbon electrode is 101-185nm, and the carbon content is 84.33%. The study shows that the AC electrode has an amorphous structure. A large number of defects lead to the increase of active sites. The specific capacitance, specific energy, and specific power of the AC electrode applied to the supercapacitor are 110 F/g, 15, 28 W/kg, and 36, 69 W/kg, respectively.

2.3.1.2 | *Using different activation processes to improve the electrochemical performance of AC*

Using jatropha oil cake as raw material, SanKari and Vivekanandhan[45] increased the specific surface area of the original carbon from 71.5 (CC) and 48.1 m^2/g (HTC) to 678.1 (CC) and 746.7 m^2/g (HTC) through the chemical activation process of KOH. The results show that the specific surface area and pore structures are improved obviously. The electrochemical properties of activated biochar obtained by conventional and hydrothermal carbonization processes were studied. The results showed that the specific capacitance of activated biochar obtained by conventional and hydrothermal carbonization processes was 145.76 and 174.78 F/g, respectively, and the energy density was 5.28 W/kg (CC) and 6.49 W/kg (HTC), respectively, at the power densities of 248.6 and 265.09 W/kg. Inal et al.[46] used 85% (WT) H_3PO_4 solution and anhydrous K_2CO_3 as chemical activators to prepare AC (AC-h and AC-k). The results show that the AC prepared by K_2CO_3 activation has a more uniform microporous structure and less surface oxygen groups, thus reducing the internal resistance and achieving good electrochemical reversibility. At the same current density, AC activated by K_2CO_3 has higher specific capacitance (the highest specific capacitance of AC-k and AC-h electrodes is 203 and 123 F/g, respectively). Sun et al.[47] prepared dual activated porous carbons with a large specific surface area (833 m^2/g), high cycle performance (specific capacitance maintained 94.2% after 10,000 cycles), and unique bimodal pore structure composed of micropores (1.8 nm) and mesopores (4.5 nm) by KOH (double activation) at high temperature. The special layered porous structure makes the AC electrode not only have the high energy storage of micropores but also have the high-rate performance of mesopores in supercapacitors (the rate performance of 197 F/g is improved at the high current density of 10 A/g). Elmouwahidi et al.[48] prepared AC mixed with olive residue, oil, and vegetable water by KOH and H_3PO_4 activation method, and applied the materials in electrode materials of supercapacitor. At the same time, two different KOH/carbon ratios (carbonization activation and impregnation activation) were used for KOH activation. The results show that the surface area of 1626 m^2/g can be obtained by KOH activation. Although the specific surface area of the H_3PO_4 activated sample is small, it has a high capacitance value and capacitance stability. The AC electrode prepared by the H_3PO_4 activation method has a phosphorus surface group and enough micro-mesh network, so AP (the AC was prepared by impregnation of OR with H_3PO_4) has the highest retention capacity, almost 100%, 176 F/g and τ (relaxation time constant) = 1.6 s. The highest capacitance of the AC electrode is 224 F/g at 250 mA/g. After 12,500 cycles and a relaxation time constant of 2.9 s, the capacity is 91%. Shree Kesavan et al.[49] produced AC with uniform micropores in petoke by KOH activation in alkaline solution and applied it to the fabrication of microporous electrode (mAC) in the symmetric configuration of mAC||KOH||mAC and hybrid configuration of mAC||KOH||$MnCo_2O_4$. Figure 9A is a cyclic voltammogram of symmetrical capacitor structure mAC||mAC in 0.5 M H_2SO_4, 2 M KOH, and 1 M KCl aqueous solution at a scanning rate of 1 mV/s. Figure 9B is cyclic voltammetry of asymmetric hybrid supercapacitor mAC||$MnCo_2O_4$ in 2 M KOH. The results show that both symmetrical capacitors and hybrid capacitors have good cycle performance (more than 98% of the initial capacitance is retained after 2500 cycles) and excellent efficiency (99.5%). Figure 9C,D is the constant current charge–discharge curves of symmetrical capacitor mAC||mAC hybrid capacitor mAC||$MnCo_2O_4$ at different current rates. Figure 9E,F shows the cycle performance of symmetrical capacitor, mAC||KOH||MAC hybrid capacitor and mAC||KOH||$MnCo_2O_4$ at a 3 A/g current rate. The symmetrical capacitor can provide the highest specific energy of 2.98 Wh/kg at a low current rate of 3 A/g, while the hybrid capacitor can provide up to 2.64 W/kg specific energy and 6805 W/kg specific power at a high current rate of 30 A/g, and can achieve the maximum energy density and power density of 3.71 and 6805 W/kg, respectively. Quan et al.[50] synthesized active biomass charcoal with a high specific capacitance of 175.6 F/g and a high energy density of 24.39 Wh/kg by using a two-step activation process of KOH. During activation, an increase in activation temperature from 700°C to 900°C resulted in an increase in specific surface area (from 1728.66 to 2330.89 m^2/g) and total pore volume (from 0.671 to 1.914 cm^3/g).

In a word, through the improvement of the raw materials and preparation methods of AC, a large number of studies have been carried out to improve the preparation and structure of AC materials to optimize their electrochemical performance at high current densities. It provides some guidance and direction for the application of AC in the field of supercapacitors.

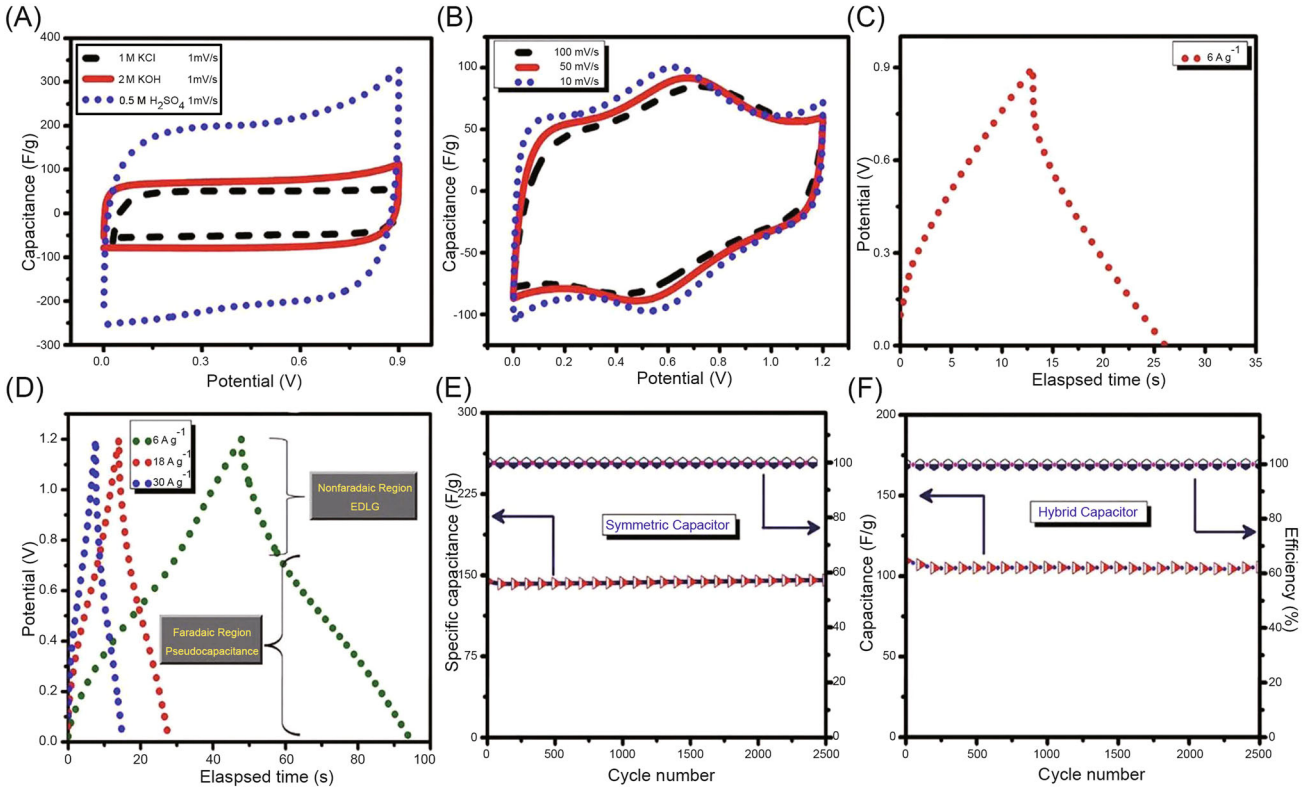


FIGURE 9 (A) Cyclic Voltammogram of symmetric capacitor configuration mAC||mAC in aqueous 0.5 M H_2SO_4, 2 M KOH, and 1 M KCl electrolytes at the scan rate of 1 mV/s. (B) Cyclic voltammogram of asymmetric hybrid supercapacitor, mAC||$MnCo_2O_4$, in 2 M KOH. Galvanostatic charge/discharge curves of (C) symmetric capacitor mAC||mAC and (D) hybrid capacitor mAC||$MnCo_2O_4$ employing 2 M KOH at different current densities. Cycling performance of (E) symmetric capacitor (mAC||KOH||mAC) and (F) hybrid capacitor (mAC||KOH||$MnCo_2O_4$) at the current density of 3 A/g. Reproduced with permission: 2018, Elsevier B.V.[49]

2.3.2 | CNCs

CNCs have a unique hollow structure, high specific surface area, and excellent chemical stability and electrical properties, so they have great application potential in lithium-ion batteries, supercapacitors, and other fields. It is worth mentioning that their nonporous outer shells are easily accessible to electrolyte ions, so CNCs have been envisioned to be promising supercapacitor electrode materials with high power density. In recent years, several researches have been conducted on the application of CNCs in supercapacitors.

Jiang et al.[51] prepared CNCs of multilayer GR with magnesium (Mg) and carbon dioxide as precursors, and further oxidized the CNCs with concentrated nitric acid (HNO_3) to graft oxygen-containing functional groups onto the surface of GR layers. The black carbon material prepared with Mg and carbon dioxide as precursors are labeled CM. The CM material is oxidized by concentrated HNO_3, which is labeled as CMN. The CNCs have high electrical conductivity and hierarchical distribution of mesoporous and macropores (the specific surface areas of CM and CMN are 806 and 866 m^2/g, respectively, before and after nitric acid oxidation). There are oxygen functional groups on the surface of the graphite layer, which makes CMN have excellent rate capability (the capacitance value reaches 96 F/g at 1000 mV/s scanning rate). Zhao et al.[52] prepared fractional nitrogen-doped CNCs (hNCNCs) using in situ MgO template method. The products have a large specific surface area, multiscale porous structure, and good wettability, as is shown in Figure 10A–C. Figure 10D indicates the coexistence of micropores (<2 nm), mesopores (2–50 nm), and macropores (>50 nm). The hNCNCs synthesized at 700°C, 800°C, and 900°C are designated as hNCNC700, hNCNC800, and hNCNC900, respectively. Figure 10E–H shows the typical electrochemical performances for the hNCNC800 and hCNC800-based supercapacitors. The optimal hNCNC800 shows a large area-specific capacitance of 17.4 $\mu F/cm^2$ and an ultrahigh mass-specific capacitance of 313 F/g at the current density of 1 A/g. The corresponding supercapacitors provide high energy density (10.90 Wh/kg) and power density (22.22 kW/kg), as well as excellent rate capability performance and cycling stability (under the condition of a high current density of 10 A/g, hNCNC800 exhibits a capacitance retention rate about 98% and a Coulombic efficiency

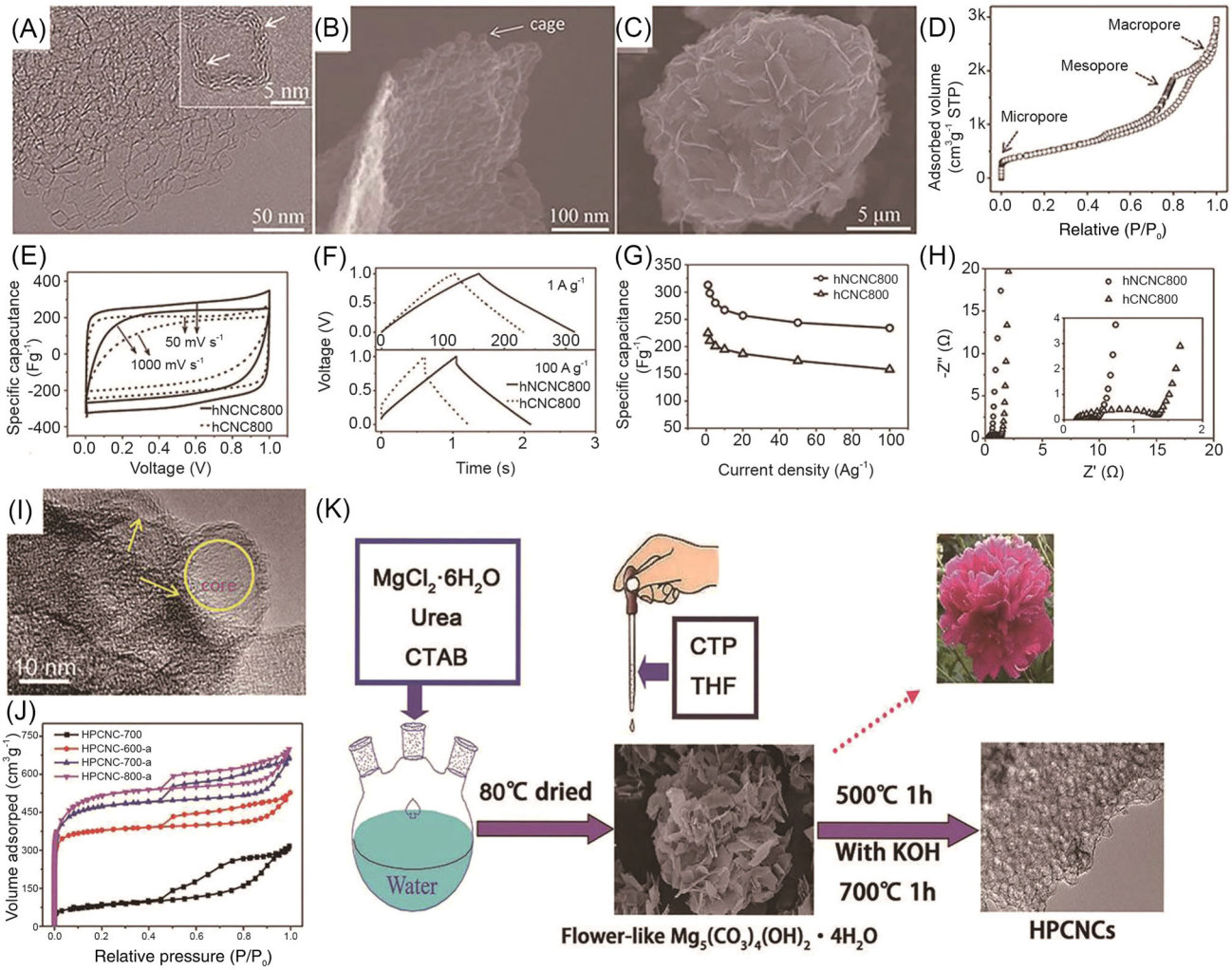


FIGURE 10 Three dimensional CNCs networks were synthesized by in situ MgO template method and different treatment methods. (A–C) Nitrogen-doped CNCs are named hNCNC. (A) TEM image of the hNCNC800. Inset is the corresponding high-resolution TEM image. Arrows indicate the broken fringes. (B,C) SEM images of the hNCNC800. (D) Nitrogen adsorption and desorption isotherm. Electrochemical characterizations of the hNCNC800 and hCNC800 in 6 M KOH electrolyte: (E) CV curves at the scan rates of 50 and 1000 mV/s; (F) CP curves at the current densities of 1 and 100 A/g; (G) gravimetric capacitances at different charge–discharge current densities. (H) Nyquist plots of hNCNC800 and hNCNC800 in 6 M KOH electrolyte. Inset magnifies the high-frequency range. Reproduced with permission: 2015, WILEY-VCH Verlag GmbH & Co. KGaA.[52] (I) TEM image of HPCNCs. (J) Nitrogen adsorption-desorption isotherms of HPCNCs. (K) Schematic diagram of the synthesis process of HPCNCs treated by carbonization and potassium hydroxide. Reproduced with permission: 2017, Elsevier B.V.[53] CNC, carbon nanocage; SEM, scanning electron microscopy; TEM, transmission electron microscopy.

about 100% after 20,000 cycles). Shao et al.[53] reported a method to prepare 3D CNCs networks by combining in-situ MgO template carbonization and KOH treatment combining with nano coating carbon precursor on flower-like basic magnesium carbonate microspheres. The samples are named HPCNC-T-a ($T = 600$, 700, or 800; "a" denotes activation by KOH). Figure 10J is a schematic of the synthesis process of HPCNCs. The TEM image of HPCNCs is shown in Figure 10I. The results show that the materials obtained by this method have interconnected 3D network structure, crosslinked CNCs (diameter size is 15–24 nm, shell thickness is 2.5–3 nm), high specific surface area (1470–1927 m^2/g), multiscale pores (macro/medium/micropores), and uniform pore size distribution. The optimal HPCNC-700-a has a larger specific capacitance of 380 F/g at 1 A/g, a higher specific capacitance of 312 F/g at 50 A/g, and a capacitance retention rate of 82% in the three-electrode system. Compared with other samples, the symmetrical HPCNC-700 still shows significant supercapacitor performance with a high specific capacitance of 288 F/g at 1 A/g and a high energy density of 9.7 Wh/kg at 500 W/kg. Bu et al.[54] reported an effective method to improve the bulk properties of carbon materials by preparing collapsed carbon nanoparticles with high density

and optimized porous structure (the collapsed CNCs [CCNC] were prepared using in situ MgO template method with benzene as carbon precursor), and they obtained three samples with decreasing sizes of mesoporous and macropore. The optimized sample achieved a high energy density of 73 W/L and a maximum stack power density of 67 KW/L in ionic liquid, maintaining 91% high stability after 100,000 cycles. Zhao et al.[55] prepared nitrogen-doped carbon nanoparticles containing graphitized shell (NGCS) by the in situ solid reaction of calcium acetate and dicyandiamide in an inert atmosphere and applied them in supercapacitors. The sample possesses a porous sheet-like structure with various spherical pores and the void is mostly around 10–20 nm in diameter, which is favorable for the transport of electrons and electrolyte ions. The specific capacitance of the NGCS electrode is 215 F/g at the current density of 0.5 A/g. In addition, the NGCS electrode has excellent multiplier performance (80% capacitance is kept at 10 A/g) and excellent cyclic stability (96.89% capacitance is kept after 5000 cycles). Wang et al.[56] used sustainable sucrose as the precursor, Ni $(NO_3)_2{\cdot}6H_2O$ as oxidant, and graphitization catalyst to form abnormal carbon nanonets with interconnected CNCs by a simple method, and this materials were used for supercapacitors with ionic liquid. The supercapacitor can provide high specific capacitance (up to 194 F/g at 1 A/g), superior rate capability (maintaining 68% capacitance at 70 A/g), and low I_R drop (0.685 V at 70 A/g). In addition, even when the ultrahigh power density is 61.250 kW/kg, the energy density can be maintained at 56.1 W/kg.

CNCs have unique structure and performance advantages in supercapacitor applications. However, the CNCs are usually macro-scale powder, and thus they have to be mixed with a binder to assemble the supercapacitors. The existence of the binder is adverse to the device's performance. CNCs obtained by traditional methods are difficult to form a binder-free film for supercapacitor application. However, how to construct CNCs-based films without 1D and 2D carbon nanomaterials to improve the effective space utilization of materials is still the bottleneck of the current research on CNCs-based films.

Zhang et al.[57] developed a colloidal film-assisted CVD method to synthesize the carbon micro-spheres films composed of CNCs. The binder-free carbon film is flexible and tough, which is advantaged for the assembly of the flexible supercapacitors. Benefitting from the composite of nano-micro 0D structures, the performance of the film is remarkably improved, and corresponding supercapacitor exhibits the ultrahigh area-specific capacity. At the current density of 5 mA/cm^2, the area-specific capacity can be 903 mF/cm^2. When the current density increases to 500 mA/cm^2, the area-specific capacity can be 729 mF/cm^2.

In addition, some carbon nanostructures, such as porous carbon, carbon nanofibers, and carbon microspheres have good nanostructures and have great application prospects in the field of electrochemistry. Khan et al.[58] prepared biomass-derived porous carbon (TWPC) from tea waste through carbonization, acidification, and KOH activation. The prepared hierarchical and tubular TWPC has a high specific surface area (1610 m^2/g), high specific capacitance (332 F/g), and good cycle performance (with a very low capacitance decay rate of 2.2% over 100,000 cycles at an ultrahigh current density of 100 A/g). Li et al.[59] prepared large micropore-dominant carbon with flaxseed residue as raw material, which achieved high surface area (3230 m^2/g) and high specific capacitance (369 and 398 F/g in KOH and H_2SO_4 electrolyte, respectively). The super electric container assembled with samples has a high energy density (61.2 Wh/kg at a power density of 468.8 W/kg) and good cycle performance (after 10,000 times of charge and discharge, the capacitance retention rate reaches more than 98.1%). Liu et al.[60] prepared porous activated carbon nanosheets (ACNS) by carbonizing waste polypropylene (PP). The prepared nanocomposites have a high specific surface area (3200 m^2/g) and high specific capacitance (349 F/g). In addition, the energy density of the prepared symmetrical supercapacitor is as high as 23 Wh/kg.

In short, CNTs with 1D structure have relatively regular pore structure, large specific surface area, and high conductivity and chemical stability. However, the limited specific surface area of CNTs affects the wide application of CNTs to a certain extent. At the same time, CNTs are usually easy to bend and wind, resulting in agglomeration. GR with a 2D structure has a large specific surface area, high electrical conductivity, and stable thermal and chemical properties. GR material will appear spontaneous re-accumulation in the process of preparation and repeated charge and discharge, which makes the theoretical value of electrochemical properties deviate greatly from the actual value. AC has the advantages of good conductivity, large specific surface area, and stable electrochemical performance. CNCs with a 3D structure has the advantages of a multiscale pore network, large specific surface area, uniform pore size distribution, good conductivity, and so on. However, due to the limited energy storage mechanism, the specific capacitance of pure carbon materials is low. In recent years, a large number of methods have been studied to improve the electrochemical performance of carbon nanomaterial supercapacitors. The following two methods are summarized: (1) preparation of composite materials; and (2) the introduction of heteroatoms are introduced to form heteroatom-doped carbon materials. Table 1 lists the performance comparison of advanced carbon-based materials mentioned in this paper.

TABLE 1 Properties of advanced carbon-based materials.

Material	Preparation method	Specific capacitance	Cycling life	Energy density (power density)	Ref.
Single carbon material					
CNTs	In situ synthesis	272 mF/cm^2 at 0.5 mA/cm^2	100% after 5000 cycles	-	[23]
GR	Buried-protection KOH activation technology	316.8 F/g at1 A/g	92.5% after 2000 cycles	-	[28]
AC	Hard template method	428.8 F/g at 0.25 A/g	98.5% after 20,000 cycles	11.2 Wh/kg	[61]
CNCs	In situ MgO template method	313 F/g at 1 A/g	100% after 20,000 cycles	10.90 Wh/kg (22.22 kW/kg)	[52]
Composite of carbon materials and metal compounds					
$NiCoMn(OH)_6$/CNT	Simple hydrothermal method	2136.2 F/g at 1 A/g	77% after 2000 cycles	-	[62]
NiCo-LDH/RGO	In situ growth and hydrothermal method	1675 F/g at 1 A/g	62.2% after 1000 cycles	49.9 Wh/kg (3747.9 W/kg)	[63]
CNTs@NiCo-LDH	Hydrothermal and electrodeposition methods	176.33 mAh/g at 1 A/g	90.22% after 5200 cycles	37.38 Wh/kg (800 W/kg)	[64]
$NiSe_2$@CNT	Rapid microwave process in 2 min	980.5 F/g at 1 A/g	82% after 9000 cycles	25.61 Wh/kg (810 W/kg)	[65]
Composite of metal organic framework (MOFs) materials and carbon materials					
Ni-CO LDH/GNR	Solvent thermal method	1765 F/g	80% after 2000 cycles	749 W/kg (25.4 W/kg)	[66]
NPMOF	Direct discourse	220 F/g	99.1% after 10,000 cycles	-	[67]
Composite of carbon material and conductive polymer					
PANI-SRPG	In situ oxidation polymerization	939.96 F/g at 1 A/g	98.46% after 5000 cycles	145 Wh/kg (17578.13 W/kg)	[68]
DMC/PANI	In-situ polymerization	985 F/g at 0.5 A/g	82% after 5000 cycles	32 Wh/kg (125 W/kg)	[69]
Carbon/carbon composites					
PRGO/CNTs	The vacuum filter and solvothermal methods	236 F/g at 0.5 A/g	-	-	[70]
GO/NCs	In situ ring-opening polymerization process coupled with KOH activation technique	405.6 F/g at 1 A/g	95.8% at 5000 cycles	38.6 Wh/kg (180 W/kg)	[71]
CMK-3/CNTs	Ultrafast microwave synthesis	315.6 F/g at 1 A/g	99.32% at 10,000 cycles	-	[72]
N-CP-CF	Atomic layer deposition technology and pyrolysis	300 F/g at 0.5 A/g	-	20.8 Wh/kg (10,000 W/kg)	[73]
LEC	Liquefaction technology	288 F/g at 0.2 A/g	97% after 3000 cycles	93.73 Wh/kg (850 W/kg)	[74]

TABLE 1 (Continued)

Material	Preparation method	Specific capacitance	Cycling life	Energy density (power density)	Ref.
Ternary complex					
CC@T-Nb_2O_5@MnO_2	Two-step hydrothermal method	319 F/g at 0.2 A/g	85.7% after 2000 cycles	31.76 Wh/kg (2250 W/kg)	[75]
MnO_2/AC/GR	The self-limiting growth method	813.0 F/g at 1 A/g	~98.4% after 1000 cycles	33.9 Wh/kg (319.3 W/kg)	[76]
MnO_2/CQDs/GA	CQDs are used as a mediator to connect MnO_2 and GA	721 F/g at 1 A/g	92.3% at 10,000 cycles	38.2 Wh/kg (1 kW/kg)	[77]
SWCNTs/RuO_2/Pin	In situ oxidation polymerization	1203 F/g at 1 A/g	95% after 10,000 cycles	33 Wh/kg (5000 W/kg)	[78]

Abbreviations: AC, activated carbon; CNC, carbon nanocage; CNT, carbon nanotube; GR, graphene.

3 | BINARY COMPLEXES

3.1 | Composite of carbon materials and metal compounds

Metal compounds, such as CO-Co_3O_4,[79] MnO_2,[80] CoS_2,[81] $NiCo_2O_4$,[82] and NiO, have been widely used in the field of supercapacitors. Metal compounds as electrode materials have high specific capacitance, but because of the poor conductivity of metal compounds, the cycle stability and rate capability are poor. Carbon nanomaterials have excellent electrochemical stability. Therefore, there are related researches combining the advantages of metal compounds and carbon nanomaterials to prepare the high-performance composite electrode materials. Zou et al.[79] prepared the CO-Co_3O_4 core particles encased in CNTs shell (hereinafter referred to as Co-Co_3O_4@CNTs-NC) by simple pyrolysis and hydrogen peroxide oxidation of melamine formaldehyde (MF) resin and cobalt acetate composite in a nitrogen atmosphere, and the results show that the prepared sample exhibits excellent electrochemical performance. When the current density is 1 A/g, it can provide high specific capacitance (823.4 F/g), and the capacitance retention rate is 93.6% after 10,000 cycles. In addition, asymmetrical dual-battery supercapacitors with Co-Co_3O_4@carbon nanotubes-NC as anode and reduced GO as cathode exhibit a high energy density of 46.7 Wh/kg at 1601.1 W/kg. Zhou et al.[80] successfully prepared porous carbon nanosheets (PCNs) by using one-step activation and carbonization of natural hollow tubular dandelion villi. Figure 11B shows the preparation process of porous carbon nanosheets derived from the dandelion fluffs by one-step activation and carbonization treatment. The dandelion villi with hollow tube structure are composed of arranged nano cellulose, which is permeated by a simple activator (KOH) activating the porous interconnected carbon nanosheets of the dandelion villi. After being coated with manganese dioxide (MnO_2), the MnO_2/PCNs composite still shows a porous interconnected structure, as shown in Figure 11A. As shown in Figure 11C, the porous interconnect GR-like structure of the AC material is helpful for the electrolyte penetration and electron transfer, improving the electrochemical performance. The electrochemical performances of MnO_2/PCNs composite are characterized in 1 M Na_2SO_4 electrolyte in three-electrode system (Figure 11D–F). The CV curves of MnO_2/PCNs composite (Figure 11D) at various scan rates (5–100 mV/s) show a mirror symmetry and regular rectangle in shape with no obvious redox peaks, presenting the typical double layer of the PCNs and pseudocapacitive behavior of the MnO_2. The asymmetric supercapacitor with manganese dioxide (MnO_2) as the positive electrode was prepared by in situ microwave deposition. Among them, conformal coating MnO_2 on PCNs can promote ion diffusion and electron

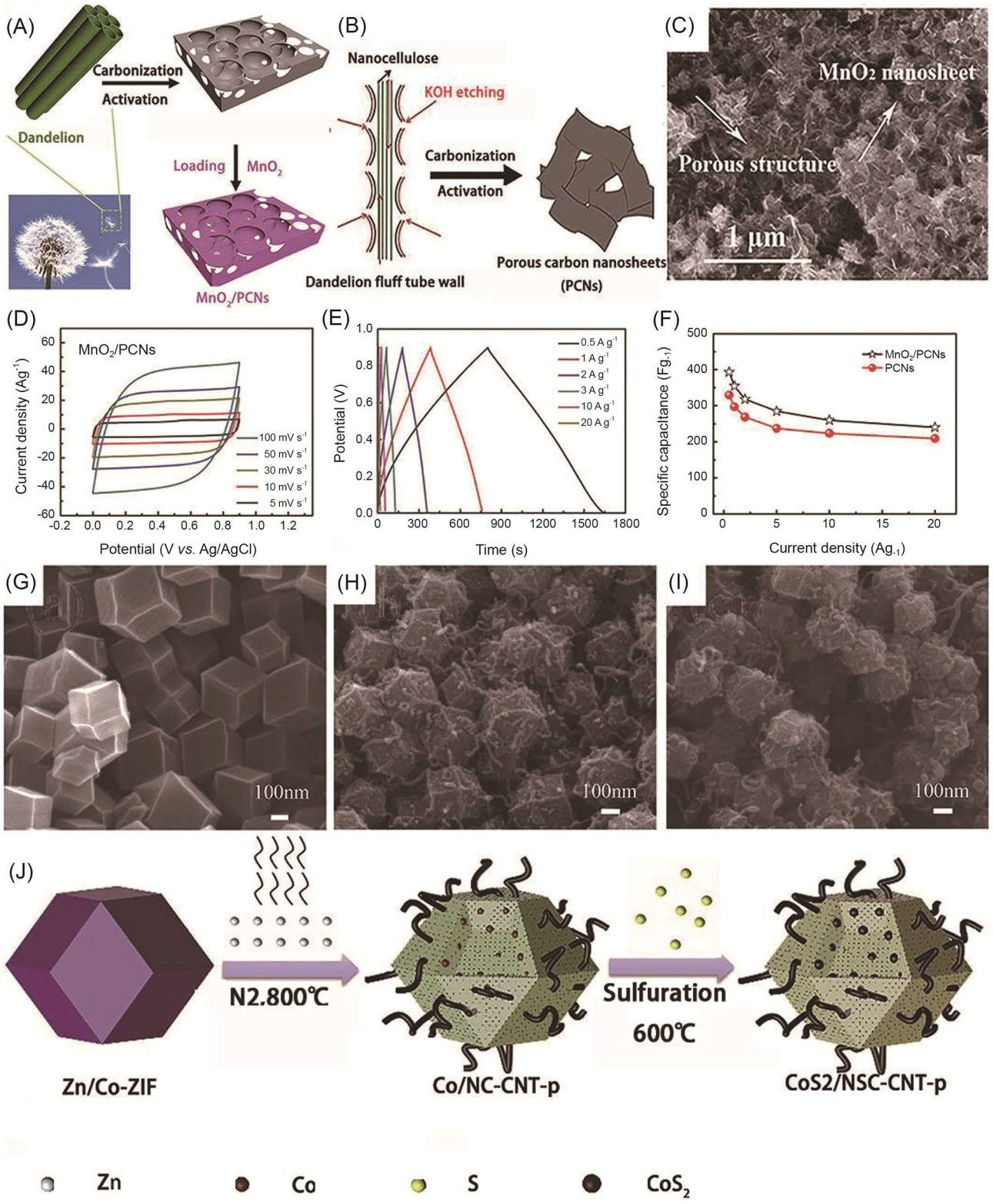


FIGURE 11 Composite of carbon materials and metal compounds. (A) Preparation process diagram of MnO_2/PCNs composites. (B) Schematic of the preparation of porous carbon nanosheets. (C) SEM image of MnO_2/PCNs composite, showing a close contact between the PCNs and the MnO_2 nanoflakes. (D) CV curves of MnO_2/PCNs composite at various scan rates. (E) Galvanostatic charge/discharge curves of MnO_2/PCNs composite at various current densities. (F) Specific capacitances of MnO_2/PCNs composite at various current densities. Reproduced with permission: 2018, Elsevier B.V.[80] SEM images of (G) Zn/Co-ZIF precursor, (H) Co/NC-CNT-p, and (I) CoS_2/NSC-CNT-p. (J) Schematic of the formation process of CoS_2/NSC-CNT-p. Reproduced with permission: 2019, Elsevier Ltd.[81] PCN, porous carbon nanosheet; SEM, scanning electron microscopy.

transport, which is helpful to improving rate performance. The research shows that the assembled asymmetric supercapacitors based on PCNs and MnO_2/PCNs composite materials have an energy density as high as 28.2 W/kg when the power density is 899.36 W/kg, and the capacitance retention rate is 89% after 10,000 cycles. Lei et al.[81] prepared the N, S-doped porous carbon loading CoS_2 nano-composite (CoS_2/NSC-CNT-p) by using zinc/cobalt-based zeolite imidazole skeleton as the precursor by two-step (carbonization and vulcanization) method. Figure 11J illustrates the synthesis procedure of CoS_2/NSC-CNT-p. According to the microstructure of CoS_2/NSC-CNT-p shown in Figures 11G,I, the CNTs-decorated CoS_2/NSC-CNT-p maintained the rhombic dodecahedral structure of the precursors, and CNTs were rooted onto the nanocomposite surface. The prepared CoS_2/NSC-CNT-p electrode has good electrochemical performance, including high specific capacitance (635.8 F/g, 1 A/g), good rate performance (544.2 F/g, 10 A/g), and long-term cycling stability (88.0% after 2000 cycles). In addition, when the power density is 0.71 kW/kg, the energy density of the CoS_2/NSC-CNT-p/AC asymmetric supercapacitor reaches 14.1 Wh/kg, and its capacitance remains at 92.2% after 2000 cycles within the potential range of 0-1.4 V. Jin et al.[82] successfully prepared a 3D elastic sponge composed of single-walled carbon nanotubes/graphene (SWNT-RGO-S) in an open environment within 20 s using an ultra-fast and simple flame combustion method, and they further deposited layered $NiCo_2O_4$ on the SWNT-RGO-S scaffold through hydrothermal treatment and annealing treatment. The compressed $NiCo_2O_4$/SWNT-RGO-S electrode has a high weight capacitance of 2050 F/g and a volume capacitance of 1200 F/cm^3 and has high cyclic stability after 6800 cycles at a current density of 20 A/g with a capacitance retention rate of 115.3%. The current densities increase from 2 to 80 A/g, and the capacitance retention rate is 73.2%. In addition, a high-performance asymmetric supercapacitor with $NiCo_2O_4$/SWNT-RGO-S as the positive electrode and activated polyaniline-derived carbon (APDC) as the negative electrode was prepared. The mass and volume energy density of the device were 53.5 Wh/kg and 26.9 Wh/L, respectively, and the high capacitance retention rate was 83.5% after 10,000 cycles. Kim et al.[83] prepared thermoelectric 2D tungsten disulfide (WS_2)/SWCNH nanocomposite by physically mixing 2D WS_2 wafer and Dali-like single-walled carbon nanohorns (SWCNHs), and then annealing with HFIHS system. With the increase of SWCNHs content, the conductivity of nanocomposites increased significantly, while the Seebeck coefficient decreased slightly with the increase in carrier concentration and mobility. Combining the conductivity and the Seebeck coefficient, the WS_2/SWCNH (0.1) power factor reaches 128.41 W/mK^2 at 780 K. In addition, the thermoelectric excellence (zT) value of 0.017 (the original WS_2) was significantly increased to 0.027 (the WS_2/SWCNH). Nguyen et al.[84] prepared $NiCo_2O_4$ nanoparticles mesoporous carbon composites (C/$NiCo_2O_4$) which have an amorphous structure and spinel structure. Due to the synergistic effect, the CS of C/$NiCo_2O_4$ is higher than that of original $NiCo_2O_4$ or carbon. The current density of C/$NiCo_2O_4$ composites is 204.28 F/g, and the CS of carbon and $NiCo_2O_4$ are 25.06 F/g and 178.78 F/g, respectively. When the current density is 2 A/g, C/$NiCo_2O_4$ has high capacitance retention of 90.35% after 3000 cycles of charge and discharge. Shang et al.[62] prepared nickel cobalt manganese/CNT composites (NiCoMn(OH)$_6$/CNT) by a simple hydrothermal method. The NiCoMn(OH)$_6$/CNT composites show a specific capacity of 2136.2 F/g at 1 A/g and still maintain a specific capacity of 1914 F/g at 10 A/g, showing excellent rate capacity. In addition, the composite maintained 77% specific capacity after 2000 cycles, showing good cycle stability. The asymmetric supercapacitor assembled with NiCoMn(OH)$_6$/CNTs as cathode material and AC as anode material material also has good electrochemical properties. The specific capacity is 150.88 F/g at 1 A/g and 81.17 F/g at 20 A/g, retaining 53.8% of the initial specific capacity. Zhang et al.[85] used the seeds of Toona sinensis as a template to obtain STS source carbon (STSC) as the cathode and anode substrates of battery supercapacitors. The prepared STSC has a large specific surface area (1031.6 m^2/g) and high specific capacitance (210.0 F/g). The specific capacitance of Ni-Co layered double hydroxide/STSC (Ni-Co LDH/STSC) prepared by hydrothermal method is 992.2 F/g at 1 A/g. Patil et al.[86] grew the ternary nanohybrid structure of RGO-$ZnCo_2O_4$ cauliflower modified by gold nanoparticles on carbon cloth by one-step hydrothermal method (Au@RGO-$ZnCo_2O_4$). The prepared Au@RGO-$ZnCo_2O_4$ composite supercapacitor has high power density (2.121 kW/kg), high energy density (31 Wh/kg), and good capacitance retention (97.01% after 5000 cycles). Zhang et al.[63] prepared reduced graphene oxide (GO) supported nickel-cobalt layered double hydroxide nanosheets (NiCo-LDH/RGO) as electrode materials for supercapacitors. The prepared nanocomposites have high capacitance (1675 F/g) and good rate performance (the capacitance remains 83.8% at 10 A/g). Zhu et al.[64] prepared hierarchical well-aligned core-shell CNTs@NiCo-LDH nanotube arrays on carbon fibers by a simple hydrothermal and electrodeposition method. The specific capacity of CNTs@NiCo-LDH is 176.33 mAh/g when the current density is 1A/g. In addition, the assembled asymmetric supercapacitor CNTs@NiCo-LDH||ZIF-8 derived carbon can provide a high energy density of 37.38 Wh/kg at a power density of 800 W/kg and maintain 90.22% capacity after 5200 cycles. Yu et al.[87] formed Fe_2O_3 conformal coating on vertically aligned CNTs by atomic layer deposition. It is found that iron oxide coating increases the regional capacitance, but too thick (30 nm) coating reduces the active area and electrochemical properties. The Fe_2O_3@CNTs

composite has the best leakage resistance, double layer and mass capacitance. Chen et al.[88] prepared a flexible conductive $Ti_3C_2TxMXene$/CNTs composite film by simple vacuum filtration of $Ti_3C_2TxMXene$ and CNTs suspension (MXene is 2D transition metal carbides and nitrides which are prepared by selective etching of the element from MAX phases). The prepared films have high capacitance (300 F/g), superior rate performance (199 F/g at 500 A/g), and good cycle stability (10,000 cycles at 20 A/g, the capacitance remains 92%). Meng et al.[89] prepared a 3D hierarchical nanostructure decorated with MoS_2 on GA nano template by surface hydrothermal method and used it as a high-performance electrode of supercapacitor. MoS_2-GA hybrid electrode has high area capacitance (0.32 F/cm^2), good rate performance, and good cycle stability (the capacitance is maintained at 92% at 5000 cycles). Suganya et al.[90] prepared electrochemically active composites of zinc vanadate ($Zn_3V_2O_8$) and nitrogen-doped multiwalled carbon nanotubes (N-MWNCT) by a simple hydrothermal method. The prepared composites have high specific capacitance (403 F/g) and good cycle performance (79% capacitance retention under 5000 cycles). Sun et al.[91] obtained InSe nanosheets from massive layered InSe materials by liquid exfoliation technology. Then, InSe/CNTs composites were prepared by adding high-conductivity CNTs into InSe nanosheets. InSe/CNTs composites have high capacity (3.48 F/cm^3), good mechanical properties (93.2% capacitance at 180° bending), and long-period stability (88.3% capacitance after 10,000 cycles). Zheng et al.[65] prepared $NiSe_2$ nano sheet@carbon nanotubes composite materials in 2 min by rapid microwave process ($NiSe_2$@CNT). The optimum $NiSe_2$@CNT electrode can display a high specific capacitance of 980.5 F/g. In addition, an asymmetric supercapacitor is assembled with the positive electrode and active carbon (AC) as a negative electrode, which can provide an energy density of 25.61 Wh/kg at a power density of 810 W/kg. Liu et al.[92] prepared 3D core-shell structure N-CNTs@CoNi-LDH composites with CoNi layered double hydroxide as shell and N-doped carbon-coated CNTs as core by in-situ growth method. The optimized N-CNTs@CoNi-LDH electrode showed good rate performance (80% retention of 20 A/g) and excellent electrochemical stability (retention of 93% after 10,000 cycles).

3.2 | Composite of MOF materials and carbon materials

As a new type of electrode material, MOF material is widely used in electrochemical energy storage devices. MOF is widely used in supercapacitor electrode materials because of its diverse structure, adjustable chemical composition, and large specific surface area.[93,94] At the same time, the application of MOF in supercapacitor electrode materials is also limited due to its poor conductivity.[95] Combining MOF with carbon materials to form MOF-derived carbon matrix materials to improve the conductivity of materials has become a research hotspot. Jin et al.[66] prepared carbon nanorods (CNR) and graphene nanorods (GNR) derived from the MOFs by a solvent thermal method. Then, Ni-CO layered double hydroxides/CNR (Ni-CO LDH/GNR) and LDH/GNR composites for supercapacitors were synthesized by a simple coprecipitation method. Studies have shown that the Ni-CO LDH/GNR composite material has a high specific capacity (1765 F/g), great rate capability (when the current density increases from 1 to 20 A/g, the capacity retention rate is 68%), and excellent cyclic stability (the capacity retention rate is 83% after 2000 charge and discharge cycles). In addition, the asymmetric supercapacitor (ASC) with Ni-CO LDH/GNR as the positive electrode and AC as the negative electrode was prepared. The ASC devices have good electrochemical performance. When the power density is 749 W/kg, the high energy density is 25.4 W/kg. After 5000 cycles of charge and discharge, the specific capacity retention rate is 96%. Gu et al.[67] synthesized a new nonporous zinc-based metal-organic framework (NPMOF) from rigid nitrogen-containing ligands. Then, the prepared NPMOF was carbonized directly to prepare porous carbon material (NPMOF-800). The prepared NPMOF-800 has a high capacitance of 220 F/g and extremely large surface area normalized capacitance of 57.7 μF/cm^2. In addition, the capacitance retention of the symmetrical double electrode device prepared with NPMOF-800 after 10,000 charge–discharge cycles is 99.1%. Wang et al.[96] prepared porous metal cobalt organic framework (PCN) with 4,4′, 4″-s-triazine-2,4,6-triyltribenzoic acid as skeleton material, which was then used to fabricate carbon-supported hybrid electrode (CNFs/PCN). In addition, an alkaline battery supercapacitor hybrid device (BSH) was prepared with CNFs/PCN as the positive electrode and AC as the negative electrode. The results show that in the voltage range of 0–1.5 V, when the power density is 749 W/kg, the maximum energy density of the PCN||AC BSH device is 16.0 Wh/kg, exhibiting good electrochemical performance. Ramachandran et al.[97] prepared cerium metal-organic skeleton composites (Ce-MOF/GO and Ce-MOF/CNT) by wet chemical method. Ce-MOF/GO composites have high specific capacitance (2221.2 F/g), and the energy density is 111.05 Wh/kg when the current density is 1 A/g.

3.3 | Composite of carbon material and conductive polymer

As an important electrode material of supercapacitors, the conductive polymer has the advantages of simple

processing, easy control of film thickness, large specific capacity and capacitance, and fast energy transmission speed.[98] However, it has the disadvantage of poor cycle life. In recent years, carbon materials and conductive polymers have been combined to improve the electrochemical performance of electrode materials. Zhou et al.[99] proposed a simple electrochemical method to prepare expanded graphite (ExGP), which can provide a large increase of contact points at the active material/collector interface. The polyaniline-carbon nanotube/surface expanded graphite (PANI-CNT/ExGP) composite electrode with a high specific capacitance of 826.7 F/g was prepared by co-deposition of polyaniline-carbon nanotube (PANI-CNT) composite on ExGP substrate. The flexible solid-state supercapacitors based on the PANI-CNT/ExGP electrodes have high flexibility and excellent electrochemical performance such as high power performance, superior energy and power characteristics (7.1 kW/kg at the energy density of 12.0 Wh/kg), and good cycle stability (capacitance retention rate of 77.6% after 3000 cycles). Lu et al.[100] prepared the hollow carbon microsphere (HCS) materials with a porous structure with a lychee shape and diameter of ~193 nm, and used them as the core framework for polypyrrole (PPy) growth. Then the PPy was evenly coated on the outer surface of the HCS to form a fluffy PPy shell. Finally, the hollow carbon microsphere@polypyrrole (HCS@PPy) composite material was successfully prepared. The preparation process and microstructure of HCS@PPy composite material are shown in Figure 12A. The HCS@PPy composite possesses a fluffy PPy thin layer with a thickness of 17 nm and keeps perfect spherical morphology. Compared with HCS and pure PPy in KOH aqueous solution, the specific capacitance of the HCS@PPy composite electrode is significantly improved because of the capacitor combination of HCS's bilayer capacitance and the Faradaic capacitance of PPy. At the current density of 1 A/g, the specific capacitance of HCS@PPy composite material is as high as 508 F/g, which is much higher than that of HCS (237 F/g). In addition, the HCS@PPy asymmetric supercapacitor shows a high energy density of 46 W/kg at a power density of 350 W/kg. At the high power density of 5600 W/kg, the energy density of the device is still 19.6 W/kg. Wu et al.[101] prepared nitrogen-doped porous carbon (NC) and partial poly (2,2′-dithiocarbidine) (PDTDA) composites (NC/PDTDA) by in-situ polymerization, which can be used as electrodes of supercapacitors in alkaline electrolytes. Figure 12B is a schematic diagram of NC/PDTDA composite preparation. NC/PDTDA-n is named according to the mass ratio of NC to PDTDA, and when the mass ratio of NC to PDTDA is 1:n, it is named NC/PDTDA-n. The experimental results show that when the mass ratio of NC to PDTDA is 1:2 (NC/PDTDA-2), the specific capacitance is the highest, and when the current density is 1 A/g, the specific capacitance is 490.5 F/g. Moreover, the asymmetric supercapacitor is also assembled with an extended operating voltage window of 1.4 V in PAM-PVA-KOH electrolyte. It exhibits an energy density of 13.49 Wh/Kg at a power density of 699.8 W/Kg. Ahirrao et al.[68] successfully synthesized solar-reduced porous graphene (SRPG) and polyaniline (PANI) nanocomposites by in situ oxidation polymerization. This unique branched structure enhances the porosity and surface area of the resulting PANI-SRPG, which facilitates the ion diffusion and charge storage processes. After 5000 galvanostatic charging–discharging (GCD) cycles, the capacitance of the PANI electrode is 555.92 F/g and the capacitance retention rate is only 69.26%. The PANI-SRPG electrode has high capacitance (939.96 F/g), high energy density (145 W/kg), high power density (17,578.13 W/kg), and good stability (98.46%). Pourreza et al.[69] prepared defective mesoporous carbon/polyaniline nanocomposites (DMC/PANI) based on defective mesoporous carbon (DMC) and polyaniline (PANI). The prepared DMC/PANI material has high specific capacitance (985 F/g at 0.5 A/g) and excellent cycle performance (82% of the specific capacitance is retained after 5000 GCD measurement at a high current density of 5 A/g). In addition, in a symmetrical supercapacitor, the sample obtained specific energy of 32 Wh/kg at a specific power of 125 W/kg. Acharya et al.[102] prepared Cr (VI)-based AC/polyaniline nanocomposites by using waste-AC and polyaniline. The prepared nanocomposites showed a high specific capacitance of 219.6 F/g and 77% medium cycle stability after 5000 charge/discharge cycles at 1 A/g current density. Moreover, the sample achieved a high energy density of 60.8 Wh/kg in an asymmetric device (organic electrolyte). Gupta et al.[103] successfully prepared the polyaniline/reduced graphene oxide (PRGO) composite hydrogels loaded with no adhesive carbon cloth. The PRGO composite hydrogel@carbon cloth (CC) obtained high specific capacitance ~235.32 F/g in 1 M H_2SO_4. Wang et al.[104] prepare nitrogen-containing hierarchical carbon nanosheets (HGPC-A) using the polyvinyl alcohol/polyaniline (PVA/PANI) hydrogels as precursors. The prepared HGPC-A has an interconnected nanosheet structure and rich hierarchical porous channels, which is conducive to high charge storage and ion penetration and transmission. The HGPC-A||HGPC-A symmetrical supercapacitor has a superb cycling durability of 88.5% over 10,000 times and a power storage capacity of 7.0 Wh/kg. Li et al.[105] Prepared hierarchical porous CNFs (HPCNFs) from polyacrylonitrile-co-acrylic acid (P(AN-CO-AA)) and terephthalic acid (PTA). The vacancy caused by the degradation of the AA fragment will produce micropores and increase the content of heteroatoms in the material, especially transforming part of N-P with low redox activity into N-P with high redox activity. The prepared HPCNFs have a

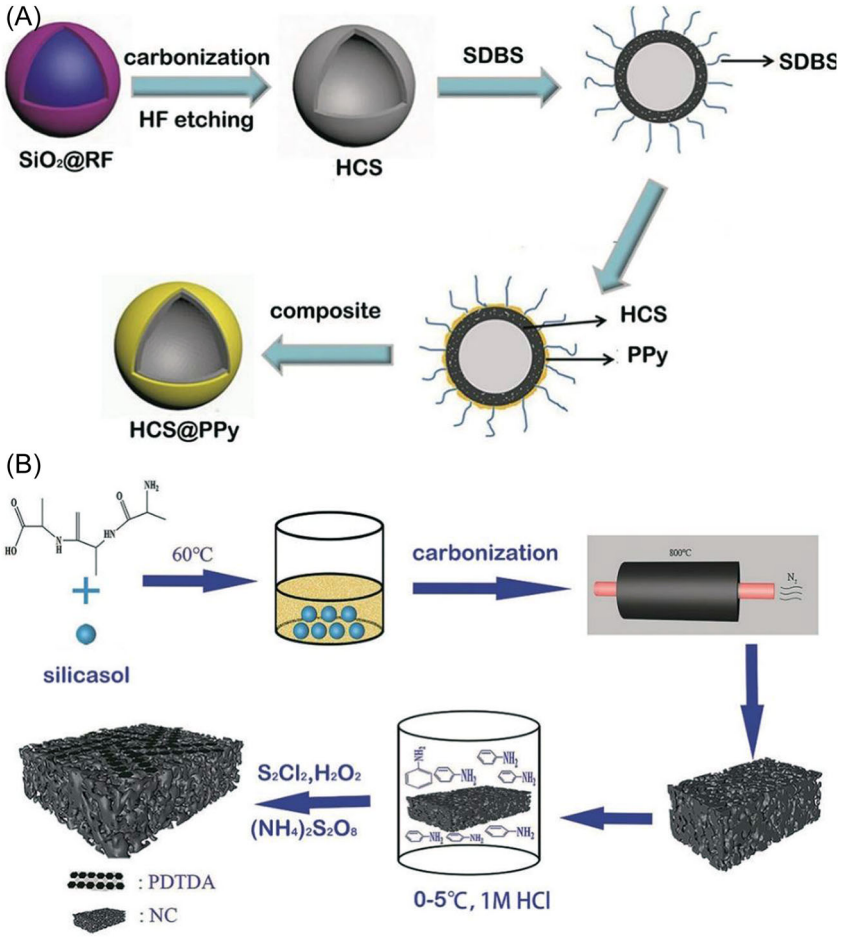


FIGURE 12 Composite diagram of carbon materials and conductive polymers. (A) Schematic illustration of synthesis procedure of HCS@PPy composite. Reproduced with permission: 2018, Elsevier Ltd.[100] (B) Schematic diagram of NC/PDTDA composite preparation. Reproduced with permission: 2021, Springer.[101]

high specific surface area (406 m^2/g) and high specific capacitance (327 F/g). Fan et al.[106] prepared an excellent redox-active polyvinyl alcohol-Li_2SO_4-1-butyl-3-methylimidazolium bromide-carbon nanotube gel polymer electrolyte (PVA-Li_2SO_4-BMIMBr-CNTs GPE). Ionic liquid bmimbr is not only used as a redox additive but also used as a plasticizer. In addition, the addition of CNTs can increase ionic conductivity and inhibit self-discharge. The prepared material can reach an energy density of 43.1 Wh/kg as well as retain 87.9% capacitance after 10,000 times of charge and discharge.

3.4 | Heteroatom-doped carbon materials

Due to the poor rate performance and low specific capacitance of carbon materials, heteroatom doping modification of carbon materials is one of the commonly used methods to improve the properties of carbon materials. Doping heteroatoms into carbon materials can effectively improve the properties of carbon materials, such as increasing the specific surface area of carbon materials, improving the conductivity of carbon materials, and optimizing the surface micropores of carbon materials.[107] In the field of supercapacitors, heteroatom-doped carbon materials can effectively combine electric double-layer capacitance and pseudocapacitance to effectively improve the energy density of supercapacitors.[108] It has important application value in the field of supercapacitor. In recent years, the preparation technology and doping methods of heteroatom-doped carbon materials have been explored to obtain heteroatom-doped carbon materials with excellent electrochemical properties. Wang et al.[109] successfully prepared N, O, and P-doped activated porous carbon with aqueous carbon derived from biomass waste durian as a precursor. The prepared AC electrode can provide up to 184 F/g at 0.5 A/g. In addition, in the redox electrolyte, the sample can obtain a specific capacitance of 560 F/g at 2 A/g. Subramani et al.[110] prepared N and B double doped porous carbon (NBPC). The NBPC material has high specific capacitance (375 F/g at 2 A/g current density in 1 M H_2SO_4), high specific surface area (809 m^2/g), high power density (15 kW/kg), and high energy

density (48.4 Wh/kg). Wang et al.[61] prepared N-doped mesoporous carbon material (CNM) by hard template method. The prepared sample has the highest specific capacitance of 428.8 F/g (0.25 A/g) and good cycle stability in the three-electrode system (the original capacitance of CNM is still 98.5% after 20,000 cycles in the three- and two-electrode systems). John et al.[111] synthesized open nitrogen-doped carbon nanotubes (N-doped CNTs) through the pyrolysis of acetylene/ammonia (C_2H_2/NH_3) mixture on lanthanum/Nickel ($LaNi_5$) alloy catalyst and subsequent 3 M HNO_3:H_2SO_4 acid mixture treatment. Among them, the traditional CVD method was used. The results show that, compared with N-doped CNTs, the open-end N-doped CNTs have higher electron conductivity, which significantly improves the rate capacitance of N-doped CNTs (the calculated capacitors of N-doped CNTs and open-end N-doped CNTs are 42 and 146 F/g, respectively). Using dimethyl disulfide as a carbon source, Kim et al.[112] synthesized sulfur-doped carbon nanotubes (S-CNTs) by CVD and purified them to obtain purified S-CNTs (P-S-CNTs) with a diameter of 30-50 nm and an S content of 0.65 at%. The electrode with P-S-CNTs exhibited the highest specific capacitance at a high discharge current density of 100 mA/cm^2 (120.2 F/g). Yu et al.[113] prepared the steam-assistant heteroatoms of sulfur and phosphorus dualdoped graphene film(s-SPG) by ice template and thermal activation methods. The s-SPG shows good pseudocapacitance behavior in flexible electrochemical capacitors. The results show that the porous s-SPG film-integrated flexible device has high specific capacitance (169 F/g), rate capability (91.7%), cycle stability (the specific capacitance retention rate of s-SPG is 92.5% after 2000 discharge/charge cycles), and good flexibility (no obvious change of specific capacitance is found even at 120° bending angle). Zhang et al.[114] prepared the 3D reduced graphene hydrogels (RGHs) through an efficient and facile strategy by employing three types of carbohydrates (glucose, fructose, and sucrose) as reducing agents in an aqueous solution of GO with ammonia (samples are expressed as FRGHs, GRGHs, and SRGHs, respectively). The excellent porous structure and N doping make the samples have high capacitance (153.5, 145.0, and 150.3 F/g at 0.3 A/g for FRGHs, GRGHs, and SRGHs, respectively), excellent rate capability (61.4%, 61.5% and 46.9% of the capacitors are kept at 20 A/g), and good cycle durability (97.1%, 96.6% and 92.8% of the capacitors are, respectively, kept at 1 A/g after 4000 cycles). In addition, the energy density of symmetrical supercapacitors based on RGHs reaches 3.63, 4.10, and 3.44 Wh/kg at a current density of 0.1 A/g for FRGHs, GRGHs and SRGHs. Miao et al.[115] prepared N/B/O-doped porous carbon scaffolds (CPLS) by auxiliary annealing pre-polymerization of ionic liquid [ABA-co-MA] [PA] network and changing the monomer ratio in amine blends. The prepared samples have a high specific surface area (2629 m^2/g) and high specific capacitance (359 F/g at 0.5 A/g). In addition, the symmetrical supercapacitor loaded with CPLS produces a high-energy output of 116 Wh/kg at 400 W/kg and long service life (98.2% retention after 10,000 cycles). Wang et al.[116] constructed an independent flexible electrode composed of a hierarchically porous N-doped welded carbon nanofiber networks (HPNWC) through electrospinning and in-situ ion-exchange reaction. Using all carbon networks as electrodes results in high specific capacitance, excellent rate performance, and long-term electrochemical stability. In addition, the prepared flexible quasi-solid-state devices still show stable electrochemical stability under severe bending. Du et al.[117] prepared N-HMCS with 3-aminophenol formaldehyde (AF) resin spheres as carbon precursors by an improved solution capture method. The prepared N-HMCS has high specific capacitance (the specific capacity of the two-electrode system is 332 F/g when the current density is 0.5 A/g), high energy density (17.1 Wh/kg), and good capacitance retention performance (after 10,000 cycles at 2 A/g, N-HMCS shows a good capacitance retention rate of 87.9%). Song et al.[118] prepared hydrangea-like heteroatoms-doped carbon (HHPCs) with a high surface area doped with heteroatoms. HHPCs solid-state symmetrical supercapacitors with $EMIMBF_4$ gel electrolyte can provide a high energy density of 101.2 Wh/kg.

3.5 | Carbon/carbon composites

Although carbon-based materials have many advantages, they also have disadvantages, such as uneven pore size distribution, low specific surface area utilization, and low specific capacitance.[3] To improve the performance of electrode materials, composite materials, which can combine the advantages of different types of electrode materials, are good options. Among them, using carbon/carbon composite material as an electrode material is a good method to improve the performance of the electrode material of a supercapacitor.

Chee et al.[119] prepared a composite by binding GR nanoplatelets to carbon nanofibers using one-step solution method based on electrospinning technology and applied it to supercapacitors. The microstructure of carbon nanofiber/graphene nanoplatelets (CNF-GNP) is shown

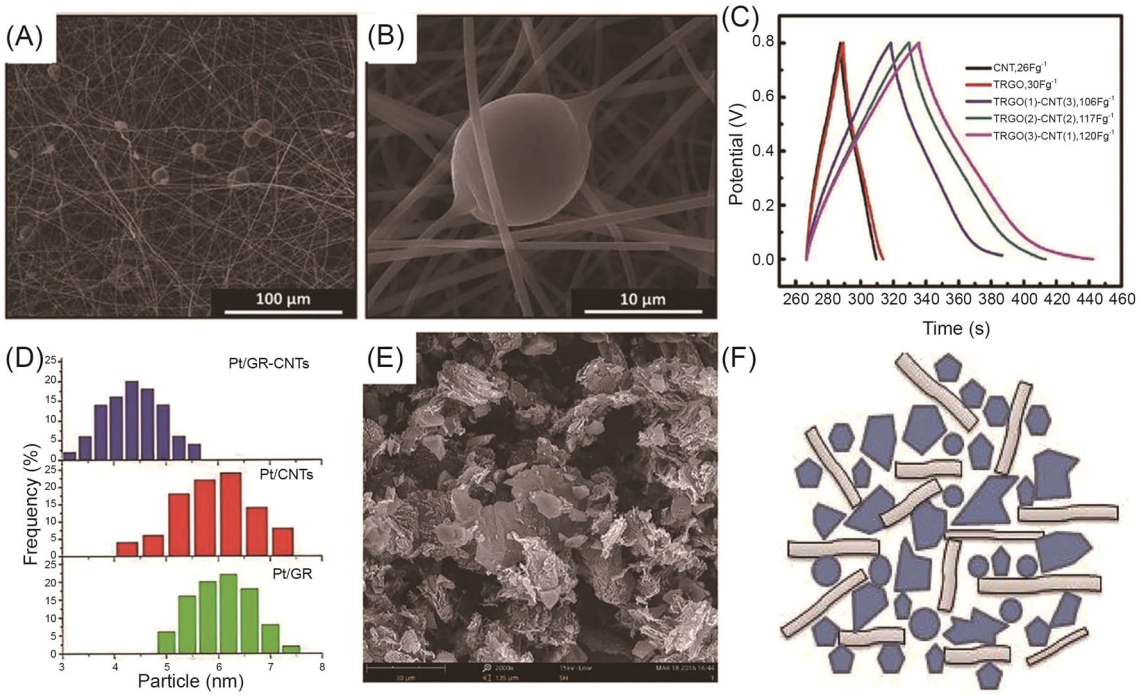


FIGURE 13 Synergism of binary composites. FESEM images of (A) CNF-GnP (1 mg/mL) and (B) magnified image showing GnP suspended within a nanofiber strand. Reproduced with permission: 2017, Elsevier B.V.[119] (C) Galvanostatic cycling with potential limitation (GCPL) results of the samples. Reproduced with permission: 2018, Korean Physical Society.[120] (D) The histograms of Pt particle size distribution of different carbon-based samples. Reproduced with permission: 2018, Elsevier Ltd.[121] (E) SEM images of 2.5% ACG. (F) Schematic illustration of the conducting network of 2.5% ACG composite. Reproduced with permission: 2017, Springer Science Business Media Dordrecht.[122] FESEM, field emission scanning electron microscopy; SEM, scanning electron microscopy.

in Figures 13A,B, and the CNF-GNP has a unique morphology. Compared with that of CNF materials, the specific capacitance of the nanofiber is significantly increased to 86.11 F/g, which is twice the increment of the original structure. In addition, after 1000 continuous charge and discharge cycles, the capacitance retention rates of all the GR nanoplate-enhanced samples were above 90%, independent of the GNP concentration. Ghanashyam et al.[120] prepared thermally reduced graphite oxide and carbon nanotube (TRGO-CNT) composite and studied the influence of different weight ratios between thermally reduced graphite oxide (TRGO) and CNT on the electrode material properties. TRGO-CNT samples with three different weight ratios are called TRGO (2) -CNT (2), TRGO (3) -CNT (1), TRGO (1) -CNT (3), respectively. The obtained capacitances are 26, 30, 106, 117, and 120 F/g for CNT, TRGO, TRGO (1) -CNT (3), TRGO (2) -CNT (2), and TRGO (3) -CNT (1), respectively, as shown in Figure 13C. The results show that the composites with more TRGO have better performance in electrochemical tests. Zhou et al.[121] prepared a GR-CNTs aerogel electrode for supercapacitors. The average particle sizes of Pt NPs are estimated from Figure 13D to be approximately 4.3, 6.8, and 4.7 nm for Pt/GR-CNTs, Pt/GR, and Pt/CNTs, respectively. This is mainly because the CNTs assembled on the surface of GR act as a barrier layer to prevent the further refilling of the sheet. Ideally, a good integrated 3D structure is formed. It is found that the addition of CNTs to GR aerogel can effectively prevent the re-accumulation of GR sheets and provide a 3D interconnected porous structure and large accessible surface area for better dispersion of Pt nanoparticles. In 6 M KOH solution, the GR-CNTs aerogel electrode has a high specific capacitance of 375 F/g, and the capacity retention rate was 88% (at 10 A/g) and 94.8% (at 1 A/g after 5000 cycles), respectively. At a current density of 1 A/g, the energy density reaches a high value of 46.5 Wh/kg, while the power density is 132 W/kg. When the current density is increased to 10 A/g, the energy density can remain at 15.2 Wh/kg and the power density is 4815.1 W/kg. Niu et al.[123] prepared lightweight 3D graphene/carbon nanotube (3DG/CNT) composites by two-step CVD method. The 3DG/CNT composite has a layered structure in which the CNTs are effectively embedded in the GR foam layer. On the one hand, the GR foam can provide a supporting platform for the CNTs. On the other hand, CNTs can reduce the influence of GR layer defects on electron transfer rate and improve the conductivity in the direction of interconnection. By providing more ion and electron transport pathways, the layered structure with a nano-interconnect

network further improves the electrochemical performance of nanocomposites. The 3DG/CNTs composite material has 197.2 F/g high specific capacitance and an excellent capacity retention rate of 93% after 1000 cycles, which shows that it has high cycle stability. Adusei et al.[124] prepared a 3D GR-CNT hybrid fiber (3DGCNT) by continuously coating CNT fiber with a nickel catalyst and then growing 3D GR flakes in the fiber through CVD. The 3DGCNT electrode has high energy density (12.93 W/kg and 14.54 Wh/cm^2 at current density 1 A/g and 1 mA/cm^2, respectively) and high power density (1350.25 W/kg and 1.37 mW/cm^2 at current density 1 A/g and 1 mA/cm^2, respectively). The PANI-3DGCNT device also demonstrated long life and cyclic stability by maintaining a high capacitance retention rate of 98.4% in 2000 charge and discharge cycles. Ye et al.[125] prepared an integrated and omnidirectional fractal tree-like N-G/CNTs composite. Among them, CNTs grow on metal nanoparticles as a "branch," and GO as a "leaf" is covalently combined with the matrix by CVD. The specific surface area of N-G/CNTs composite is 190.66 m^2/g, and its pore size distribution is 4–6 nm. Yan et al.[70] prepared partially reduced graphene oxide/carbon nanotubes (PRGO/CNTs) films by vacuum filtration and solvothermal method. The prepared film has a high specific capacitance of 236 F/g. In addition, the assembled PRGO/CNTs||$NiCo_2O_4$ asymmetric supercapacitor can provide an energy density of 18.8 Wh/kg and a capacitance retention rate of 99.5% after 5000 cycles at 5 A/g. Liu et al.[126] prepared a novel woven fabric electrode for the seamless connection of GR/nanotube. By adding conductive polymer to the seamless GR/nanotube hybrid electrode fabric, the synthesized all-solid-state supercapacitor has a high specific capacity of 164 mF/cm^2.

Not only does the combination of GR and CNTs effectively improve the properties of electrode materials, but the combination of GR and other carbon materials also shows excellent advantages. Lin et al.[127] prepared nitrogen-doped graphene/carbon nanohorns composite (NGLC) as electrode materials for supercapacitors by one-step co-pyrolysis of GO, carbon nanohorns (CNHs), low-cost lignin sulfonate, and urea. CNHs are inserted between GR layers, which serve not only as spacers but also as bridges between the GR sheets. The specific surface area of NGLC is as high as 465.4 m^2/g due to the introduction of carbon nanoangles into the GR nanosheets and the loose nanostructure of NGLC. The NGLC has excellent comprehensive electrochemical performance, with a specific capacitance of up to 363 F/g at a current density of 1 A/g and a capacitance retention rate of 93.5% after 5000 cyclic voltammetry (CV) cycles. Wan et al.[71] prepared a GO/NCs nanocomposite with phenolphthalein, urea, and formaldehyde as raw materials. In the 6 M KOH electrolyte, the GO content of the GO/NCs nanocomposite electrode is 1.29 wt%, and the maximum specific capacitance is 405.6 F/g at the current density of 1.0 A/g. It also shows better rate performance (267.8 F/g at 40 A/g) and cycle durability (95.8% capacitance retention at 5000 cycles) than activated polybenzoxazine (PBM)-based nanopores without GO. In addition, the GO/NCs symmetric supercapacitor device prepared in 1 M Na_2SO_4 can achieve a working voltage of 1.8 V and show a high energy density of 38.6 Wh/kg at 180 W/kg, while maintaining a power density of 19.9 Wh/kg at 32.4 kW/kg. Wang et al.[122] reduced GO to GR and used it as the building blocks and spacers of AC to prepare a type of graphene-containing composite material (ACG) for an interconnected conductive network. The microscopic structure of the ACG composite is shown in Figure 13E, and it can be observed that GR sheets are interspersed in the AC particles. Owing to the bridge role of GR, AC particles can be easily connected with each other. In figure 13F, there ACG composite. It has been shown to have better electrochemical performance than AC, including higher specific capacitance (284 F/g, current density 0.5 A/g), better multiplier behavior (70.7% retention), and more stable cycling performance (no capacitor attenuation even after 2000 cycles). Liu et al.[128] prepared porous carbon/few-layered graphene (PC/FLG) composites by carbonization and KOH activation of the obtained FLG and polyrvinylpyrrolidone (PVP). The prepared PC/FLG composites have a high specific surface area (SSA) (3008 m^2/g), hierarchical microporous and mesoporous structures (dominant pores in the range of 1-5 nm), high specific capacitance (up to 340 F/g), and good cycle stability (94.4% capacitance retention after 10,000 cycles). At the same time, the symmetrical supercapacitor has a high energy density of 10.9 Wh/kg (based on the total mass of the electrode material) and excellent energy density retention, even at high power density. Li et al.[129] prepared layered porous carbon/graphene composites (PCGs) with large specific surface area, abundant micropores/mesoporous, great conductivity, and strong chemical interaction between porous carbon particles and GR by using soluble low-molecular-weight phenolic resin as a carbon source in molten KCl. Due to the bridging effect of GR and the strong chemical interaction between GR and carbon particles, carbon particles can be easily connected to each other. The PCG composite has excellent capacitances in the three-electrode system, including higher specific capacitance (341 F/g at a current density of 0.5 A/g), better power capacity (69.5% at a current density of up to 20 A/g), and more stable cycling performance in a 6 M potassium hydroxide aqueous electrolyte (95.2% capacitance retention after 5000 cycles). Meanwhile, in the dual-electrode battery,

PCG has high capacitance (174 F/g at a current density of 0.5 A/g) and good cycling stability (capacitance retention rate of 91.8% after 5000 cycles). Yang et al.[130] prepared a 3D carbon-based aerogel (TOCN/RGO(CTRGO) aerogel) electrode material by freeze-drying TOCN/GO gel and subsequently carbonizing at high temperature. Compared with 750°C carbonization, 1100°C carbonization produces more pores and, a larger specific surface area structure, which improves the electron and ion transport efficiency. The electrochemical property of carbonized TOCN/RGO(CTRGO) aerogel is 398.47 F/g at the current density of 0.5 A/g. In addition, the capacitance remains 99.77% after 10,000 charge–discharge cycles, showing excellent cycle stability.

Of course, CNTs and other carbon materials can also get better properties. Wan et al.[131] prepared nitrogen-doped porous carbon/CNTs (CNT@CZIF-2) composite materials with large specific surface area (287 m^2/g), high specific surface area (324 F/g), and good cycling stability (93.5% capacitance retention rate after 1000 cycles in alkaline water electrolyte solution) by in-situ growth of nitrogen-rich ZIF-8 nanoparticles onto CNT and carbonization at 800°C. Fu et al.[132] synthesized CNT with N-doped mesoporous carbon (CNT@N-PC) composite materials using resorcol-formaldehyde resin as carbon source, ionic liquid (ILS) as template and nitrogen source, and tetraethyl orthosilicate (TEOS) as an auxiliary agent. Using ILS modified CNT with nitrogen, TEOS promotes the creation of more abundant mesoporous structures. The CNT@N-PC obtained consists of a CNT nucleus and mesoporous carbon particles, forming a 3D network structure, such as "Dew Spider web." The material has a specific surface area of 857 m^2/g, uniform pore size distribution (3.0 nm), and an appropriate N content (at 4.9%). The CNN@N-PC has a high specific capacitance (244 F/g at 1 A/g), good multiplier performance, and good capacitance retention (92.5% after 5000 cycles) when used as a supercapacitor electrode, indicating potential applications in high-performance supercapacitors. Yan et al.[72] prepared a hierarchical rambutan carbon composite with ordered mesoporous carbon as the core and CNTs as the shell. The synthesized ordered mesoporous carbon CMK-3/CNTs composites have high specific capacitance (315.6 F/g at 1 A/g), rate performance (214.6 F/g at 50 A/g), and cycle durability (10,000 cycles, 99.32%). Kang et al.[133] filtered the stable double-wall carbon nanotubes (DWNTs) suspension into a film and then chemically activated the film with sodium hydroxide to prepare DWNT/AC composites. The composite has strong mechanical strength and high conductivity. When the current density is 100 mV/s, its specific capacitance reaches 141.5 F/g.

The synergistic effect of other carbon materials can also make the electrode materials obtain excellent electrochemical properties. Zhao et al.[73] prepared carbon particle and carbon foam composite (N-CP-CF). The obtained samples have a hierarchical porous structure, large specific surface area (538 m^2/g), and excellent electrochemical properties (high specific capacitance of 300 F/g and high energy density of 20.8 Wh/kg). Moreover, the N-CP-CF composite can provide stable capacitance (250 F/g) and energy density (17.36 Wh/kg) under large deformation (25% of the original thickness). Zhang et al.[74] prepared Larch-based carbon composites with excellent electrochemical properties from Larch sawdust. The material shows high specific capacitance (288 F/g), energy density (93.73 Wh/kg), and power density (850 W/kg) at a current density of 0.2 A/g in 1 M KOH electrolyte. At the same time, the material has good rate performance and stability (the capacitance retention rate exceeds 97% after 3000 cycles).

4 | TERNARY COMPLEX

To further improve the electrochemical performance of electrode materials on the basis of binary composites, increasing the number of components is a clever idea.[133] Zhang et al.[134] prepared carbon nanotube/graphene (CNT/G) composite sponge by in situ partial decompression, and then they electrically polymerized the polypyrrole onto the sponge to form CNT/graphene/polypyrrole (CNT/G/PPy) ternary composite sponge. The specific capacitance of CNT/G/PPy composite material is increased from 4 to 225 F/g. At the same time, CNT/G/PPy sponge retains the internal conductive network, showing excellent capacitance performance. In addition, cycling tests showed that the capacitance of the CNT/G/PPy composite sponge remains at 90.6% after 1000 cycles of 20 mV/s. Compression tests showed that the capacitance remained 92% (at a strain of 50%) under compression. Wang et al.[75] prepared the complex layered nanostructure of T-Nb_2O_5@MnO_2 supported by carbon cloth. The microstructure of carbon cloth@T-Nb_2O_5@MnO_2 (CC@T-Nb_2O_5@MnO_2) is shown in Figure 14. The supercapacitive properties of MnO_2 nanosheets can be accelerated by T-NB_2O_5 nanorods, and the carbon cloth (CC) backbone can improve the electronic conductivity of the composite. The CC@T-Nb_2O_5@MnO_2 has a high specific capacitance (319 F/g at 0.2 A/g) and good cycling stability (85.7% capacitance retention after 2000 cycles) for the hierarchical nanostructure and reasonable synergistic effects. In addition, the energy density of the asymmetric supercapacitor with CC@T-

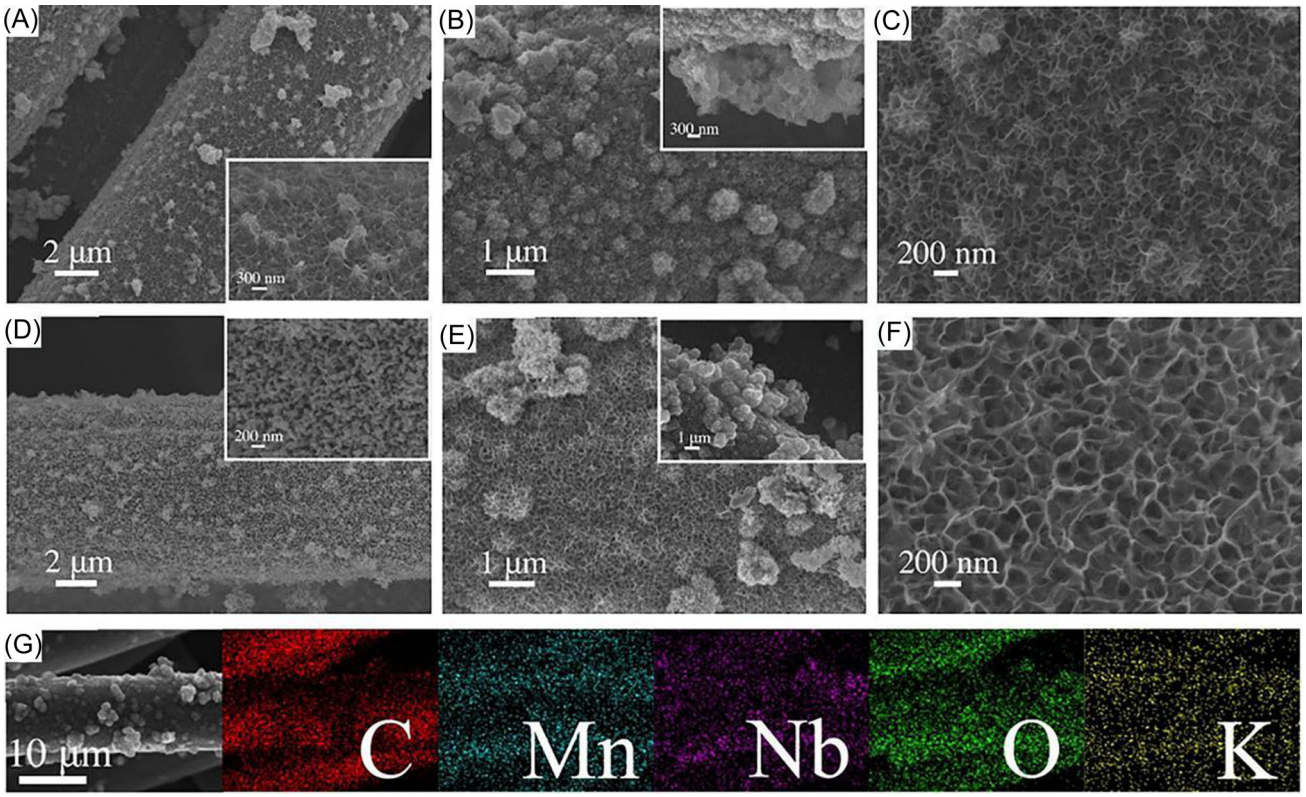


FIGURE 14 Low and high magnification SEM images of (A) carbon cloth@Nb_2O_5, (B,C) carbon cloth@Nb_2O_5@MnO_2, (D) carbon cloth@T-Nb_2O_5, and (E,F) carbon cloth@T-Nb_2O_5@MnO_2. (G) EDS mappings of carbon cloth@T-Nb_2O_5@MnO_2. Reproduced with permission: 2017, Elsevier Ltd.[75] EDS, energy dispersive spectroscopy; SEM, scanning electron microscopy.

Nb_2O_5@MnO_2 nanocomposite as the positive electrode and activated graphite oxide as the negative electrode is 31.76 Wh/kg, and the maximum power density is 2250 W/kg. Tseng et al.[76] synthesized a ternary composite material composed of MnO_2, AC, and GR. Through the redox reaction of $KMnO_4$ on the AC interlayer, the layered porous MnO_2 top layer of the ternary composite is realized by the self-limiting growth method. The ternary MnO_2/AC/GR composite electrode has the advantages of high specific capacitance (813.0 F/g), good electrochemical stability, and cycle stability (capacitance retention rate ~98.4% after 1000 cycles). In addition, the energy density and power density of the solid-state supercapacitor based on the ternary composite electrode are 33.9 and 319.3 W/kg, respectively, which shows the prospect of the energy storage application. Lv et al.[77] used carbon quantum dots (CQDs) to connect MnO_2 and graphene to synthesize MnO_2/CQDs/graphene composite aerogel (MnO_2/CQDs/GA), in which the CQDs are used as a mediator to improve the electrochemical properties of the electrode materials. The composite electrode has high specific capacitance (721 F/g at 1 A/g), good capacitance retention (89.2% capacitance retention at 20 A/g), and excellent cycle stability (92.3% capacitance retention at 10,000 cycles). High-performance symmetrical supercapacitors are fabricated with MnO_2/CQDs/GA electrodes. The device shows that the energy density is 38.2 Wh/kg when the corresponding power density is 1 kW/kg. When the power density reaches 20 kW/kg, the energy density can still be maintained at 18.65 Wh/kg. Sengottaiyan et al.[135] synthesized a unique indium oxide/carbon nanotubes/reduced graphene oxide (In_2O_3/CNT/RGO) ternary nanocomposite by hydrothermal method. The glass-carbon electrodes modified with In_2O_3/CNT/RGO nanocomposites have high specific capacitance (1273 F/g [5 mV/s] and 948 F/g [1 A/g]), good capacitance retention (±75% observed at a high scanning rate of 200 mV/s), and excellent cyclic stability (no capacity loss after 5000 cycles). Xie et al.[136] assembled the RGO network on CNT-Fe_3O_4 thin film by electrophoresis and constructed a flexible solid-state supercapacitor device based on two symmetric independent CNT-Fe_3O_4-RGO electrodes. The solid supercapacitor has a specific capacitance of 275.6 F/g and a superior energy density of 36.7 Wh/kg. After 10,000 charge and discharge cycles, it retained more than 92.9% of the initial capacitance remains above 92.9%. Maity

et al.[137] prepared the ternary nanohybrid materials, using hexagonal boron nitride (BN) with various carbon-containing materials (GO, RGO, CNT) and polyaniline (PANI). It is found that the maximum specific capacitance of BN/CNT/PANI composite in 1 M KCl is 387.5 F/g when the current density is 1 A/g. When the power density of ternary composite was 400 W/kg, the high energy density of 34.44 W/kg is achieved. In addition, the ternary nanohybrid BN/CNT/PANI retains 87% of the specific capacitance after 6000 charging disharging cycle. Bonakdar et al.[138] synthesized poly-o-anisidine/carbon nanotube/reduced graphene oxide (POA/CNT/RGO) nanocomposites by in-situ polymerization. The specific capacitance of POA/CNT/RGO composite is 142 F/g. The specific capacitance of POA/CNT/RGO composite is lower than that of POA/RGO, but much higher than those of pure POA and POA/CNT. After 500 cycles, the initial capacitance of POA/CNT/RGO only reduced by 7%, while those of POA/RGO and POA/CNT composites reduced by 50% and 60%, respectively. Zhang et al.[139] successfully synthesized carbon/PDA/PMA hybrid structures by combining polydopamine (PDA) and phosphomolybdic acid (PMA), and realized the double surface modification of carbon materials. These structures have superior capacitive properties in supercapacitor applications. PDA can not only be used as a connecting molecule to increase the interaction between PMA and carbon matrix but also be used as a pseudo capacitor provider. In addition, in the dual-electrode configuration, the C-PDA/PMA-1:1 sample (the mass ratio of C-PDA to PMA is 1:1) sample provides 101 F/g at 1 A/g, the 10,000 cycle performance is 108%, and the energy density is 3.5 Wh/kg at 500 W/kg (close to 3.2 times of C-blank sample which were prepared by the direct carbonization of sodium citrate at 800 °C for 2 h under nitrogen gas flow). Zhao et al.[140] prepared multistage PPy@MnO_2 core-shell nanowires by CVD-polymerization technology, which is a new approach to prepare multistage PPy@MnO_2 core-shell nanowires. After that, by constructing a hierarchical PPy@MnO_2 structure on CF, the PPy@MnO_2@CF was prepared. The prepared PPy@MnO_2@CF electrode showed a large area capacitance of 1.24 F/cm^2. Using PPy@MnO_2@CF and Fe_2O_3@CF as positive and negative electrodes, respectively, flexible solid-state asymmetric supercapacitors (FSASC) are assembled. Under the power density of 9.8 mW/cm^3, FSASC delivers the maximum energy density of 1.93 mWh/cm^3 and has a long-term life of 92.6% of the initial capacitance after 10,000 cycles. Liu et al.[141] prepared a self-supporting CoZnNiS@CNTs/RGO composite membrane. Among them, porous CNTs/RGO films are used as conductive substrates to support the vertical 2D CoZnNiS nano arrays derived from CoZn-MOFs. The CoZnNiS@CNTs/RGO composite film has high specific capacitance (1349.2 F/g) and high capacity (727.0 F/cm^3). In addition, the hybrid supercapacitor assembled by CoZnNiS@CNTs/RGO and carbon ball/RGO achieves ultrahigh energy density (60.4 Wh/kg) and excellent cycle performance (90.6% capacitance retention after 10,000 cycles). Gorduk et al.[142] prepared metal phthalocyanine/functionalized multiwall carbon nanotube/polyaniline/pencil graphite electrode (MPc/f-MWCNT/PANI/PGE) modified electrode to obtain a supercapacitor with high specific capacitance, high energy and power density, and long cycle life. The specific capacitance of the NIPc/f-MWCNT/PANI/PGE electrode (325 F/g) is higher than those of ZnPc/f-MWCNT/PANI/PGE (278 F/g), CuPc/f-MWCNT/PANI/PGE(282 F/g), f-MWCNT/PANI/PGE (162 F/g), and PANI/PGE (126 F/g). In addition, all MPc/f-MWCNT/PANI/PGE electrodes have a long cycle life and can still maintain about 100% capacitance after 1000 charge–discharge cycles. Patil et al.[143] applied 2D reduced graphene oxide (RGO) on diamond-like cubic tungsten oxide ($WO_3 \cdot 0.5H_2O$) and then modified it with plant monoclinic copper sulfide (Cu_2S), and they finally prepared 3D heterostructure RGO/$WO_3 \cdot 0.5H_2O$@Cu_2S electrodes. The prepared materials play a synergistic effect and have a high specific surface area(545.6 mF/cm^2) and high capacitance (974.4 F/g). In addition, the asymmetric pouch-type solid-state supercapacitor (APSC) has excellent cycling stability of 88% over 10000 rapid charging/discharging cycles and a short relaxation time of 0.084 s at a frequency of 11.9 Hz. Kshetri et al.[144] prepared ternary carbon hybrid nanostructures composed of carbon nanotube@graphene and carbon nanofiber (CNTs@Gr-CNF). The CNTs@Gr-CNF electrode material has high specific capacitance (521.5 F/g) and good cycle performance (the capacitance retention is 98% after 10,000 charges and discharges). Hekmat et al.[145] prepared porous carbon microspheres modified by ternary metal sulfide nanosheets with a unique hierarchical structure. Layered microspheres (HTCs) modified by ternary zinc cobalt sulfide nanosheets (NS) were directly used as the cathode of the supercapacitor. In addition, the composite of pyrolytic polyaniline nanotubes (PPNTs) and iron oxide was used as the cathode material of asymmetric supercapacitor. It has a high energy density (85 Wh/kg) and good capacitance retention (81.4% for 6000 charge–discharge cycles). Dang et al.[146] prepared 3D NiCoP/CoP heterogeneous nanosheet networks supported on nitrogen-doped CNTs by one-step phosphorization of nickel-cobalt hydroxide. The prepared N-CNTs@NiCoP/COP electrode has a high specific

capacity (152 mAh/g). In addition, the hybrid supercapacitor composed of N-CNTs@NiCoP/COP and ZIF-67 porous carbon anode has an energy density of 45.5 Wh/kg when the power density is 784 W/kg. After 10,000 cycles at 12 A/g, the retention rate is 87%. Zhu et al.[78] prepared ternary single-wall carbon nanotube/RuO_2/polyindole (SWCNTs/RuO_2/Pin) nanocomposites by oxidative polymerization of indole on prefabricated CNT/RuO_2 binary nanocomposites. The symmetrical supercapacitor with SWCNTs/RuO_2/Pin as electrode has high capacitance (1203 F/g), high energy density (33 Wh/kg), and good cycle performance (the retention rate is 95% after 10,000 cycles). Mei et al.[147] hybridized metal phthalocyanine conjugated microporous polymers (MPC-CMPs) with highly conductive CNTs by a simple vacuum filtration method to prepare CoPC-CMP/CNTs composites. Flexible CoPC-CMP/CNTs show high specific capacitance (289.1 F/g) and good capacity retention (the capacitance remains 82.4% after 1350 cycles at a high current density of 10 A/g). Huang et al.[148] prepared MWCNTs/$FeNi_3$/polyaniline nanocomposites by in-situ polymerization. The newly prepared MWCNTs/$FeNi_3$/PANI ternary composites have high specific capacitance (398.1 F/g), large energy and power density (9.1 and 500 W/kg, respectively), and good cycle performance (80.9% capacity retention after 2000 charge–discharge cycles). Zhang et al.[149] developed a simple fabrication method of symmetrical TiN-TiO_2-VACNT 3D micro supercapacitor device synthesized by atomic layer deposition (ALD). Among them, atomic layer deposition (ALD) is used to deposit conformal pseudocapacitive coatings of titanium oxide (TiO_2) and titanium nitride (TiN) onto vertically aligned carbon nanotubes (VACNT) grown by CVD. The results show that the specific capacitance of the TiN-TiO_2-VACNT device (5.18 mF/cm^2) is more than 74 times higher than that of bare vacnt MSc device (0.07 mF/cm^2), which provides an idea for the development of new microscale or large-area energy storage equipment in the future.

5 | APPLICATION OF CARBON NANOMATERIALS IN HYBRID CAPACITORS

Hybrid capacitor is a new method of supercapacitor electrode design, which can effectively improve the performance of a supercapacitor.[150] One electrode of the hybrid capacitor is the supercapacitor electrode, and the other electrode is the battery electrode. As a new material in the 21st century, carbon nanomaterials have the advantages of large specific surface area and good conductivity. They are widely used in the field of hybrid capacitors. Li et al.[151] have designed a high-performance quasi solid-state sodium-ion hybrid capacitor, which is composed of Mo_2N quantum dots coupled with CNTs as anode, decoupled graded CNTs as cathodes, and gel electrolyte based on porous polyvinylidene fluoride fluor propene (PVDF-HFP) film. Among them, layered CNTs with high specific surface area and a large number of in-plane nanopores contribute to rapid and reversible anion adsorption and desorption, and greatly improve the specific capacity of the capacitor. In addition, the microstructure of low-curvature nanotube electrode with an open frame is conducive to the unimpeded penetration of electrolyte ions, so that the active materials can be used to the greatest extent. The assembled quasi solid-state sodium-ion hybrid capacitor can reach a high energy density of 100.6 Wh/kg at a power density of 117.5 W/kg. It is a potentially high-energy-density storage device. Wei et al.[152] prepared 3D porous layered carbon quantum dots (CQDS)/M_xO_y (M=Co, Ni) composite nanostructures by thermal decomposition of corresponding CQDS/$M(OH)_y$. The prepared layered porous CQDS/Co_3O_4 nanostructures have high specific capacitance (1603 F/g at 1 A/g) and good cycle performance (the capacity remains at 97.0% after 2000 cycles). In addition, CQDS/Co_3O_4||AC hybrid supercapacitors (HSCs) have high specific capacities of 210.4 F/g and 74.8 Wh/kg. Hu et al.[153] designed a high-energy-density hydrogen-ion water-based hybrid supercapacitor with $Ti_3C_2T_x$ MXene as a negative electrode and HQ/CNT as a positive electrode. The complementary potential window of the two electrodes makes the hybrid device (MXene||CNT-HQ) have a voltage window of up to 1.6 v. In addition, the hybrid supercapacitor achieves a high specific capacitance of 176 F/g and provides a high energy density of 62 Wh/kg.

6 | PROGRESS IN SUPPRESSING SELF-DISCHARGE AND CAPACITY ATTENUATION OF SUPERCAPACITORS

Self-discharge is one of the important indexes to measure the performance of supercapacitors in practical applications. The self-discharge of a supercapacitor is the phenomenon of spontaneous voltage attenuation after being fully charged. The unsatisfactory fast self-discharge will significantly attenuate the capacitance of the supercapacitor and deteriorate the cycle life of the device.[154] In recent years, researchers have done a lot of research on the mechanism and suppression strategy of self-discharge of supercapacitors and summarized the following three strategies: (1) modification of electrode materials; (2)

adjustment of electrolytes to inhibit self-discharge behavior; (3) modification of the diaphragm of supercapacitor. From the aspect of electrode materials, carbon-based electrode materials will inevitably produce oxygen-containing functional groups in the preparation process, and the concentration of oxygen-containing functional groups on the electrode surface has a great correlation with the self-discharge of the supercapacitor.[155] Therefore, controlling the concentration of oxygen-containing functional groups on the electrode surface to inhibit the self-discharge of the supercapacitor is one of the feasible methods. Zhang et al.[155] studied the self-discharge mechanism of a single-wall CNT supercapacitor and revealed the influence of surface chemistry on its self-discharge by interfering with the electrostatic interaction between electrolytic ions and the surface of a single-wall CNT. The self-discharge rate of the SWCNT supercapacitor is adjusted by simply trimming the surface chemical properties of nanotubes. The experimental results show that the reduction of functional groups on the surface of SWCNT by heat treatment can indeed inhibit self-discharge. Du et al.[156] introduced different contents of Fe/Fe_3O_4 into AC by vacuum impregnation and annealing, and systematically studied the effect of Fe doping on the self-discharge of carbon supercapacitor. The experimental results show that the self-discharge of supercapacitor decreases significantly by more than 39.7% after introducing a low content of Fe/Fe_3O_4 into AC. Li et al.[157] used the surface engineering strategy to design layered porous structures on the surface of fiber carbon-containing O/N heteroatomic functional groups and realized aqueous Zn ion hybrid supercapacitors (ZHSs) with high energy and anti-self-discharge. Hierarchical pore structure and appropriate surface functional groups make ZHSs have high energy/power density and good self-discharge resistance. In recent years, researchers have also done a lot of research on the inhibition mechanism of electrolytes on self-discharge behavior. Su et al.[158] introduced mixed liquid crystal E7 molecules into the electrolyte, which effectively inhibited the self-discharge of the supercapacitor. The results show that the supercapacitor with E7 has low self-discharge and leakage current. In the presence of E7, the 24-h open circle potential (OCP) decreased from 3 to 1.4 V, while in the absence of E7, the OCP decreased to 1.1 V. Meanwhile, in the presence of E7, the leakage current is reduced from 10 to 2.2 μA. Wang et al.[159] added sulfonate ion exchange resin to the separator to capture impurities, so as to inhibit the self-discharge of the redox-active polymer poly (3,4-ethylenedioxy-thiophene) (PEDOT) supercapacitor. The cation exchange mechanism of the modified membrane is generally effective in organic electrolytes and aqueous solutions with pH 0–14.

7 | SUMMARY AND OUTLOOK

This review compares the current research status of single carbon materials in different dimensions for supercapacitors and shows current problems. Based on the above summary, a single-carbon nanomaterial has a high specific surface area and high electrical conductivity, which can allow to fabricate electrode materials with an energy density of up to 11.20 Wh/kg. However, due to the limitation of the energy storage mechanism, the specific capacitance of carbon nanomaterials is low. Therefore, the researchers have composited carbon nano-materials and other materials with pseudocapacitance, to obtain high specific capacitance from 508 to 1756 F/g. Without compositing, the specific capacitance of single-carbon nanomaterials is only from 55 to 380 F/g. Moreover, the combination of two carbon nanomaterials with different types and structures can also improve the specific capacitance of product and coordinate the advantages of two carbon materials to obtain a high specific energy density up to 46.5 Wh/kg. To further improve the performance of binary composites, it is a relatively simple method to increase the number of components as the "bridge" between the two materials to form the ternary composites. The design and control of various carbon materials are proposed. By sorting and categorizing the research in recent years, the composites-based carbon materials for supercapacitors are systematically introduced. Therefore, in this review, the different nanostructures of carbon and different kinds of composites based on carbon were analyzed in detail. The design and control of carbon materials are to achieve improvements in their electrochemical performance. So, a deep understanding of the relationship between structure and performance can provide a guide to carbon materials with the most suitable structure for supercapacitors.

The future research of carbon materials is believed to focus on the following aspects to promote the development of supercapacitors. In the future, pure carbon electrode materials can be further studied in the following aspects: (1) it is highly desirable to study the effects of defect content, heteroatom content, and functional group content on the properties of carbon nanomaterials, and it is worth trying further to introduce defects, impurity atoms (N, P, O, etc.), and surface functional groups to customize the structure and properties of carbon electrodes. (2) Designing and constructing a conductive network to form a conductive film, such as adding spacers such as bridging agent and surfactant in the graphene layer, can effectively prevent the re-accumulation of graphene, connect the layers and construct a conductive network, and improve the conductivity of graphene materials. (3) The regularization and arrangement of carbon nanomaterials make the materials

have regular structure and good orientation, so as to improve the electrochemical performance of the electrode (4) Optimizing the preparation strategy and exploring the methods of high-quality carbon nanomaterials that can be produced on a large scale set the foundation for commercial applications. As for the types of carbon materials, it is necessary to explore and develop carbon materials with high conductivity and high specific surface area similar to graphene and CNTs. The emergence of single-type carbon materials provides more choices for the synthesis of composite carbon materials. In terms of basic theory, it is necessary to further study the relationship between material structure, composite mode, and electrochemical properties. At the same time, the application of carbon nanomaterials in hybrid supercapacitors is also briefly introduced in this paper. The configuration of a hybrid supercapacitor can effectively increase the operating voltage window of electrolytes, so as to improve the energy density of supercapacitors. The design and optimization of new carbon nanomaterials also provide a new idea for the design of hybrid supercapacitors. In terms of composite methods, there are many possibilities for further improvement and enrichment in the future.

First, the pore size and structure of carbon are designed and controlled more accurately by making full use of the combination of synthesis methods, so as to obtain carbon materials with new structures suitable for supercapacitors. Secondly, the current strategy of introducing micropores into carbon materials is very limited. It is necessary to develop new pore-forming methods to improve the existing pore-forming technologies and methods. Third, the design and control of structure should be further studied. The morphological and structural changes of different types of substances before and after synthesis were studied. According to the law of morphological and structural transformation, the carbonized structure of carbon precursors formed by these substances can be estimated, so that the design can accurately guide the synthesis of carbon materials with complex structures. Fourth, in the application, the synthesis steps should be simplified as much as possible. To make synthetic carbon materials economical, mild reaction conditions and low-cost raw materials should be used. In addition, the synthesis process is environmentally friendly and safe. Of course, while optimizing the electrode materials of carbon-based supercapacitors, we must also pay attention to the self-discharge of supercapacitors. At present, it is necessary to study the self-discharge mechanism of different carbon nanomaterials. At the same time, how to find a breakthrough in improving electrochemical performance and inhibiting self-discharge is the focus of future research. With the unremitting efforts of researchers, the design and control of carbon materials will be able to successfully produce supercapacitors with high specific capacitance and high energy density to meet the needs of energy storage devices in the future. It is believed that through continuous development and improvement, supercapacitors can be more widely used in production and life.

ACKNOWLEDGMENT

This study was supported by the Science & Technology Development Fund of Tianjin Education Commission for Higher Education (2019KJ092).

CONFLICTS OF INTEREST

The authors declare no conflicts of interest.

ORCID

Miao Zhang http://orcid.org/0000-0001-7258-1412
Xifei Li http://orcid.org/0000-0002-4828-4183

REFERENCES

1. Wu X, Liu R, Zhao J, Fan Z. Advanced carbon materials with different spatial dimensions for supercapacitors. *Nano Mater Sci*. 2021;3(3):241-267.
2. Wang J, Zhang X, Li Z, Ma Y, Ma L. Recent progress.of biomass-derived carbon materials for supercapacitors. *J Power Sources*. 2020;451:227794.
3. Wang G, Zhang L, Zhang J. A review of electrode materials for electrochemical supercapacitors. *Chem Soc Rev*. 2012; 41(2):797-828.
4. Oriti G, Anglani N, Julian AL. Hybrid energy storage control in a remote military microgrid with improved supercapacitor utilization and sensitivity analysis. *IEEE Trans Ind Appl*. 2019;55(5): 5099-5108.
5. Edwards E, Brantley C, Ruffin PB. *Overview of Nanotechnology in Military and Aerospace Applications*. John Wiley & Sons, Ltd; 2017.
6. Corcau JI, Dinca L. Fuzzy energy management scheme for a hybrid power sources of high-altitude pseudosatellite. *Modell Simul Eng*. 2020;2020:1-13.
7. Bartłomiejczyk M, Jarzębowicz L. Energy savings by application of supercapacitor storage in trolleybus supplying station-analysis of experimental results. *Czasopismo Techniczne. Elektrotechnika*. 2016;2:17-32.
8. Wang L, Wen L, Tong Y, et al. Photo-rechargeable batteries and supercapacitors: critical roles of carbon-based functional materials. *Carbon Energy*. 2021;3(2):1-28.
9. Hasan NS, Rosmin N, Nordin NM, Hassan MY. Virtual inertial support extraction using a super-capacitor for a wind-PMSG application. *IET Renew Power Gener*. 2019;13(10):1802-1808.
10. Wang P, Wang H, Zhang J, Cai X. Design and application of supercapacitor energy storage system used in low voltage ride through of wind power generation system. *Proc CSEE*. 2014; 34(10):1528-1537.
11. Karimi-Rizvandi A, Sandjareh M, Nazari MH, Ezati-Yaraziz M. A novel frequency control scheme for autonomous microgrid using cooperative application of supercapacitor-battery HESS, photovoltaics, LED lighting loads and TCLs. *IEEE Access*. 2021;9:57198-57214.

12. Teng Y, Wei J, Du H, Mojtaba M, Li D. A solar and thermal multi-sensing microfiber supercapacitor with intelligent self-conditioned capacitance and body temperature monitoring. *J Mater Chem A*. 2020;8:11695-11711.
13. Skinner B, Chen T, Loth MS, Shklovskii BI. Theory of volumetric capacitance of an electric double-layer supercapacitor. *Phys Rev E*. 2011;83(2):056102.
14. Liu Q, Zhang H, Xie J, Liu X, Lu X. Recent progress and challenges of carbon materials for Zn-ion hybrid supercapacitors. *Carbon Energy*. 2020;2(4):521-539.
15. Lim E, Jo C, Lee J. A mini review of designed mesoporous materials for energy-storage applications: from electric double-layer capacitors to hybrid supercapacitors. *Nanoscale*. 2016;8:7827-7833.
16. Vangari M, Pryor T, Jiang L. Supercapacitors: review of materials and fabrication methods. *J Energy Eng*. 2013; 139(2):72-79.
17. Liu F, He J, Liu X, et al. MoC nanoclusters anchored Ni@N-doped carbon nanotubes coated on carbon fiber as three-dimensional and multifunctional electrodes for flexible supercapacitor and self-heating device. *Carbon Energy*. 2021;3(1):129-141.
18. Zeng J, Xu C, Gao T, Jiang X, Wang X. Porous monoliths of 3D graphene for electric double-layer supercapacitors. *Carbon Energy*. 2021;3(2):193-224.
19. Rodríguez-Reinoso F, Molina-Sabio M. Activated carbons from lignocellulosic materials by chemical and/or physical activation: an overview. *Carbon*. 1992;30(7):1111-1118.
20. Xie K, Qin X, Wang X, et al. Carbon nanocages as supercapacitor electrode materials. *Adv Mater*. 2012;24(3):347-352.
21. Hussain S, Amade R, Jover E, Bertran E. Nitrogen plasma functionalization of carbon nanotubes for supercapacitor applications. *J Mater Sci*. 2013;48(21):7620-7628.
22. Shi K, Zhitomirsky I. Fabrication of polypyrrole-coated carbon nanotubes using oxidant-surfactant nanocrystals for supercapacitor electrodes with high mass loading and enhanced performance. *ACS Appl Mater Interfaces*. 2013; 5(24):13161-13170.
23. Yang J, Guo J, Guo X, Chen L. In-situ growth carbon nanotubes deriving from a new metal-organic framework for high-performance all-solid-state supercapacitors. *Mater Lett*. 2018;236:739-742.
24. Cao C, Zhou Y, Ubnoske S, et al. Highly stretchable supercapacitors via crumpled vertically aligned carbon nanotube forests. *Adv Energy Mater*. 2019;9(22):1900611-1900618.
25. Adusei PK, Gbordzoe S, Kanakaraj SN, et al. Fabrication and study of supercapacitor electrodes based on oxygen plasma functionalized carbon nanotube fibers. *J Energy Chem*. 2020; 40:120-131.
26. Fedorovskaya EO, Bulusheva LG, Kurenya AG, et al. Supercapacitor performance of vertically aligned multiwall carbon nanotubes produced by aerosol-assisted CCVD method. *Electrochim Acta*. 2014;139:165-172.
27. Childress A, Ferri K, Rao AM. Helically coiled carbon nanotubes as supercapacitor electrodes. *Carbon*. 2018;140:377-384.
28. Li Z, Zhang L, Chen X, Li B, Wang H, Li Q. Three-dimensional graphene-like porous carbon nanosheets derived from molecular precursor for high-performance supercapacitor application. *Electrochim Acta*. 2018;296:8-17.
29. Lu X, Xiang K, Zhou W, Zhu Y, He Y, Chen H. Graphene-like carbon derived from macadamia nut shells for high-performance supercapacitor. *Russ J Electrochem*. 2019;55: 242-246.
30. He D, Marsden AJ, Li Z, Zhao R, Xue W, Bissett MA. A single step strategy to fabricate graphene fibres via electrochemical exfoliation for micro-supercapacitor applications. *Electrochim Acta*. 2019;299:645-653.
31. Li Q, Horn M, Wang Y, Macleod J, Motta N, Liu J. A review of supercapacitors based on graphene and redox-active organic materials. *Materials*. 2019;12(5):703.
32. Yuan K, Xu Y, Uihlein J, et al. Straightforward generation of pillared, microporous graphene frameworks for use in supercapacitors. *Adv Mater*. 2016;27(42):6714-6721.
33. Wang H, Wang Y, Hu Z, Wang X. Cutting and unzipping multiwalled carbon nanotubes into curved graphene nanosheets and their enhanced supercapacitor performance. *ACS Appl Mater Interfaces*. 2012;4(12):6827-6834.
34. Silva AA, Pinheiro RA, Rodrigues AC, Baldan MR, Trava-Airoldi VJ, Corat EJ. Graphene sheets produced by carbon nanotubes unzipping and their performance as supercapacitor. *Appl Surf Sci*. 2018;446:201-208.
35. Bhattacharya G, Fishlock SJ, Pritam A, Roy SS, Mclaughlin JA. Recycled red mud-decorated porous 3D graphene for high-energy flexible micro-supercapacitor. *Adv Sustainable Syst*. 2020;4(4):1900133.
36. Strauss V, Marsh K, Kowal MD, El-Kady M, Kaner RB. A simple route to porous graphene from carbon nanodots for supercapacitor applications. *Adv Mater*. 2018;30(8): 1704441-1704449.
37. Huang G, Hou C, Shao Y, et al. High performance all-solid-state yarn supercapacitors based on porous graphene ribbons. *Nano Energy*. 2015;12:26-32.
38. Wang J, Ding B, Xu Y, Shen L, Dou H, Zhang X. Crumpled nitrogen-doped graphene for supercapacitors with high gravimetric and volumetric performances. *ACS Appl Mater Interfaces*. 2015;7:22284-22291.
39. Chao Y, Chen S, Xiao Y, et al. Ordinary filter paper-derived hierarchical pore structure carbon materials for supercapacitor. *J Energy Storage*. 2021;35:102331.
40. Le Van K, Thi TTL. Activated carbon derived from rice husk by NaOH activation and its application in supercapacitor. *Prog Nat Sci Mater Int*. 2014;24(3):191-198.
41. Li LJ, Wang XY, Wang SJ, et al. Activated carbon prepared from lignite as supercapacitor electrode materials. *Electroanalysis*. 2016;28(1):243-248.
42. Zhu X, Yu S, Xu K, et al. Sustainable activated carbons from dead ginkgo leaves for supercapacitor electrode active materials. *Chem Eng Sci*. 2018;181:36-45.
43. Jiang C, Yakaboylu GA, Yumak T, Zondlo JW, Sabolsky EM, Wang J. Activated carbons prepared by indirect and direct CO_2 activation of lignocellulosic biomass for supercapacitor electrodes. *Renewable Energy*. 2020;155:38-52.
44. Agus A, Farma R, Taer E. The production and characterization of activated carbon electrodes from pineapple leaf fibers for supercapacitor application. *J Aceh Phys Soc*. 2020;9(1):1-8.
45. Sankari MS, Vivekanandhan S. Jatropha oil cake based activated carbon for symmetric supercapacitor application: a comparative

study on conventional and hydrothermal carbonization processes. *ChemistrySelect*. 2020;5(4):1375-1384.
46. Inal IIG, Holmes SM, Banford A, Aktas Z. The performance of supercapacitor electrodes developed from chemically activated carbon produced from waste tea. *Appl Surf Sci*. 2015;357:696-703.
47. Sun J, Yang SH, Li SS, Cao BQ. Double-activated porous carbons for high-performance supercapacitor electrodes. *Rare Metals*. 2017;36(5):449-456.
48. Elmouwahidi A, Bailón-García E, Pérez-Cadenas AF, Maldonado-Hódar FJ, Carrasco-Marín F. Activated carbons from KOH and H_3PO_4-activation of olive residues and its application as supercapacitorelectrodes. *Electrochim Acta*. 2017;229:219-228.
49. Shree Kesavan K, Surya K, Michael MS. High powered hybrid supercapacitor with microporous activated carbon. *Solid State Ionics*. 2018;321:15-22.
50. Quan C, Su R, Gao N. Preparation of activated biomass carbon from pine sawdust for supercapacitor and CO_2 capture. *Int J Energy Res*. 2020;44(6):4335-4351.
51. Jiang L, Wang J, Mao X, et al. High-rate performance carbon nano-cages with oxygen-containing functional groups as supercapacitor electrode materials. *Carbon*. 2017;111:207-214.
52. Zhao J, Lai H, Lyu Z, et al. Hydrophilic hierarchical nitrogen-doped carbon nanocages for ultrahigh supercapacitive performance. *Adv Mater*. 2015;27(23):3541-3545.
53. Shao J, Song M, Wu G, et al. 3D carbon nanocage networks with multiscale pores for high-rate supercapacitors by flower-like template and in-situ coating. *Energy Storage Mater*. 2017;13:57-65.
54. Bu Y, Sun T, Cai Y, et al. Compressing carbon nanocages by capillarity for optimizing porous structures toward ultrahigh-volumetric-performance supercapacitors. *Adv Mater*. 2017;29(24):1700470.
55. Zhao J, Liu C, Xiang K, et al. In-situ template formation strategy for the preparation of nitrogen doped carbon nanocage with graphitic shell as electrode material for supercapacitor. *J Nanosci Nanotechnol*. 2018;18:6949-6956.
56. Wang D, Wang Y, Liu H, Xu W, Xu L. Unusual carbon nanomesh constructed by interconnected carbon nanocages for ionic liquid-based supercapacitor with superior rate capability. *Chem Eng J*. 2018;342:474-483.
57. Zhang M, Zhao N, Li X. The synthesis of carbon microspheres fim composed of nano-onions and its application as flexible supercapacitors. *Carbon Energy*. 2021;3(3):509-518.
58. Khan A, Senthil RA, Pan J, Osman S, Sun Y, Shu X. A new biomass derived rod-like porous carbon from tea-waste as inexpensive and sustainable energy material for advanced supercapacitor application. *Electrochim Acta*. 2019;335:135588.
59. Li Y, Zhang D, Zhang Y, et al. Biomass-derived microporous carbon with large micropore size for high-performance supercapacitors. *J Power Sources*. 2019;448:227396.
60. Liu X, Ma C, Wen Y, et al. Highly efficient conversion of waste plastic into thin carbon nanosheets for superior capacitive energy storage. *Carbon*. 2021;171:819-828.
61. Wang L, Sun J, Zhang H, Xu L, Liu G. Preparation of benzoxazine-based N-doped mesoporous carbon material and its electrochemical behaviour as supercapacitor. *J Electroanal Chem*. 2020;868:114196.
62. Shang Y, Ma S, Wei Y, Yang H, Xu Z. Flower-like ternary metal of Ni-Co-Mn hydroxide combined with carbon nanotube for supercapacitor. *Ionics*. 2020;26(12):3609-3619.
63. Zhang L, Cai P, Wei Z, et al. Synthesis of reduced graphene oxide supported nickel-cobalt-layered double hydroxide nanosheets for supercapacitors. *J Colloid Interface Sci*. 2020;588:637-645.
64. Zhu F, Liu W, Liu Y, She W. Construction of porous interface on CNTs@NiCo-LDH core-shell nanotube arrays for supercapacitor applications. *Chem Eng J*. 2019;383:123150.
65. Zheng Y, Tian Y, Sarwar S, Luo J, Zhang X. Carbon nanotubes decorated $NiSe_2$ nanosheets for high-performance supercapacitors. *J Power Sources*. 2020;452:227793.
66. Jin H, Yuan D, Zhu S, Zhu H, Zhu J. Ni-Co layered double hydroxide on carbon nanorods and graphene nanoribbons derived from MOFs for supercapacitor. *Dalton Trans*. 2018;47(26):8706-8715.
67. Gu Y, Miao L, Yin Y, Liu M, Gan L, Li L. Highly N/O co-doped ultramicroporous carbons derived from nonporous metal-organic framework for high performance supercapacitors. *Chin Chem Lett*. 2020;32(4):1491-1496.
68. Ahirrao DJ, Mohanapriya K, Wilson HM, Jha N. Solar reduced porous graphene incorporated within polyaniline network for high-performance supercapacitor electrode. *Appl Surf Sci*. 2020;510:145485.
69. Pourreza K, Adeh NB, Mohammadi N. In-situ grown of polyaniline on defective mesoporous carbon as a high performance supercapacitor electrode material. *J Energy Storage*. 2020;30:101429.
70. Yan K, Wu J, Wang YY, et al. An asymmetric supercapacitor based on $NiCo_2O_4$ nanosheets as anode and partially reduced graphene oxides/carbon nanotubes as cathode. *Chem Pap*. 2019;74:591-599.
71. Wan L, Du C, Yang S. Synthesis of graphene oxide/polybenzoxazine-based nitrogen-containing porous carbon nanocomposite for enhanced supercapacitor properties. *Electrochim Acta*. 2017;251:12-24.
72. Yan K, Sun X, Ying S, et al. Ultrafast microwave synthesis of rambutan-like CMK-3/carbon nanotubes nanocomposites for high-performance supercapacitor electrode materials. *Sci Rep*. 2020;10(1):6227.
73. Zhao Z, Kong Y, Liu C, et al. Atomic layer deposition-induced integration of N-doped carbon particles on carbon foam for flexible supercapacitor. *J Materiomics*. 2020;6(1):209-215.
74. Zhang Y, Chen H, Wang S, et al. A new lamellar larch-based carbon material: fabrication, electrochemical characterization and supercapacitor applications. *Ind Crops Prod*. 2020;148:112306.
75. Wang T, Le Q, Zhang J, Zhang Y, Li W. Carbon cloth@T-Nb_2O_5@MnO_2: a rational exploration of manganese oxide for high performance supercapacitor. *Electrochim Acta*. 2017;253:311-318.
76. Tseng LH, Hsiao CH, Nguyen DD, Hsieh PY, Lee CY, Tai NH. Activated carbon sandwiched manganese dioxide/graphene ternary composites for supercapacitor electrodes. *Electrochim Acta*. 2018;266:284-292.
77. Lv H, Yuan Y, Xu Q, Liu H, Wang YG, Xia Y. Carbon quantum dots anchoring MnO_2/graphene aerogel exhibits

excellent performance as electrode materials for supercapacitor. *J Power Sources*. 2018;398:167-174.
78. Zhu D, Zhou Q, Liang A, et al. Two-step preparation of carbon nanotubes/RuO_2/polyindole ternary nanocomposites and their application as high-performance supercapacitors. *Front Mater Sci*. 2020;14(9):109-119.
79. Zou Y, Cai C, Xiang C, et al. Simple synthesis of core-shell structure of Co-Co_3O_4@carbon-nanotube-incorporated nitrogen-doped carbon for high-performance supercapacitor. *Electrochim Acta*. 2018;261:537-547.
80. Zhou J, Li YJ, Huang FG, et al. High-performance asymmetric supercapacitor assembled with three-dimensional, coadjacent graphene-like carbon nanosheets and its composite. *J Electroanal Chem*. 2018;823:S981635271.
81. Lei K, Ling J, Zhou J, Zou H, Yang W, Chen S. Formation of CoS_2/N, S-codoped porous carbon nanotube composites based on bimetallic zeolitic imidazolate organic frameworks for supercapacitors. *Mater Res Bull*. 2019;116:59-66.
82. Jin F, Tong H, Lu L, et al. Honeycombed $NiCo_2O_4$ nanosheets grown on the sponge of a carbon nanotube/graphene prepared by the flame burning method with an advanced performance as a supercapacitor. *J Alloys Compd*. 2019;787:36-44.
83. Kim JH, Yu S, Lee SW. Enhanced thermoelectric properties of WS_2/single-walled carbon nanohorn nanocomposites. *Crystals*. 2020;10(2):140.
84. Nguyen NV, Tran TV, Luong ST, et al. Facile synthesis of a $NiCo_2O_4$ nanoparticles mesoporous carbon composite as electrode materials for supercapacitor. *ChemistrySelect*. 2020;5(23):7060-7068.
85. Zhang D, Guo X, Tong X, et al. High-performance battery-type supercapacitor based on porous biocarbon and biocarbon supported Ni-Co layered double hydroxide. *J Alloys Compd*. 2020;837:155529.
86. Patil SJ, Dubal DP, Lee D. Gold nanoparticles decorated rGO-$ZnCo_2O_4$ nanocomposite: a promising positive electrode for high performance hybrid supercapacitors. *Chem Eng J*. 2020;379:122211.
87. Yu P, Coll M, Amade R, et al. Homogeneous Fe_2O_3 coatings on carbon nanotube structures for supercapacitors. *Dalton Trans*. 2020;49(13):4136-4145.
88. Chen H, Yu L, Lin Z, et al. Carbon nanotubes enhance flexible MXene films for high-rate supercapacitors. *J Mater Sci*. 2020;55(3):1-9.
89. Meng Z, He X, Han S, Hu Z. Three-dimensional MoS_2/graphene hybrid aerogel as free-standing, high-performance electrode for supercapacitor. *Nano*. 2020;15(05):1210.
90. Suganya B, Maruthamuthu S, Chandrasekaran J, et al. Design of zinc vanadate ($Zn_3V_2O_8$)/nitrogen doped multiwall carbon nanotubes (N-MWCNT) towards supercapacitor electrode applications. *J Electroanal Chem*. 2020;881:114936.
91. Sun X, Chang Y, Mu C, et al. Two-dimensional layered materials InSe nanoflakes/carbon nanotubes composite for flexible all-solid-state supercapacitors. *J Mater Sci*. 2020;55(7):2947-2957.
92. Liu R, Wang Y, Sun S, Chen C, Wu X. CoNi layered double hydroxide anchored on N-doped carbon coated carbon nanotubes network with 3D Core-shell structure for all-solid-state supercapacitors. *J Electroanal Chem*. 2020;878:114571.
93. Sundriyal S, Shrivastav V, Sharma M, Mishra S, Deep A. Redox additive electrolyte study of Mn-MOF electrode for supercapacitor applications. *ChemistrySelect*. 2019;4(9):2585-2592.
94. Wang KB, Wang ZK, Liu JD, et al. Enhancing the performance of a battery-supercapacitor hybrid energy device through narrowing the capacitance difference between two electrodes via the utilization of 2D MOF-nanosheet-derived Ni@nitrogen-doped-carbon core-shell rings as both negative and positive electrodes. *ACS Appl Mater Interfaces*. 2020;12(42):47482-47489.
95. Xiong SS, Jiang SY, Wang J, et al. A high-performance hybrid supercapacitor with NiO derived NiO@Ni-MOF composite electrodes. *Electrochim Acta*. 2020;340:135956.
96. Wang K, Bi R, Huang M, et al. Porous cobalt metal-organic frameworks as active elements in battery-supercapacitor hybrid devices. *Inorg Chem*. 2020;59(10):6808-6814.
97. Ramachandran R, Xuan W, Zhao C, et al. Enhanced electrochemical properties of cerium metal-organic framework based composite electrodes for high-performance supercapacitor application. *RSC Adv*. 2018;8(7):3462-3469.
98. Snook GA, Kao P, Best AS. Conducting-polymer-based supercapacitor devices and electrodes. *J Power Sources*. 2011;196(1):1-12.
99. Zhou H, Zhi X, Zhai HJ. A facile approach to improve the electrochemical properties of polyaniline-carbon nanotube composite electrodes for highly flexible solid-state supercapacitors. *Int J Hydrogen Energy*. 2018;43(39):18339-18348.
100. Lu Q, Liu J, Wang X, Lu B, Chen M, Liu M. Construction and characterizations of hollow carbon microsphere@polypyrrole composite for the high-performance supercapacitor. *J Energy Storage*. 2018;18:62-71.
101. Wu S, Yin Y, Wei D, et al. Synthesis of nitrogen-doped porous carbon and partial poly (2, 2′-dithiodianiline) composite as advanced supercapacitor electrode materials. *J Mater Sci Mater Electron*. 2021;32:9332-9344.
102. Acharya S, Sahoo S, Sonal S, Lee JH, Mishra BK, Nayak GC. Adsorbed Cr(VI) based activated carbon/polyaniline nanocomposite: a superior electrode material for asymmetric supercapacitor device. *Compos B Eng*. 2020;193:107913.
103. Gupta A, Ohlan A, Singh K. Efficient electrode material based on carbon cloth supported polyaniline/reduced graphene oxide composites for supercapacitor application. *Indian J Pure Appl Phys*. 2021;59:68-74.
104. Wang M, Yang J, Liu S, Li M, Hu C, Qiu J. Nitrogen-doped hierarchically porous carbon nanosheets derived from polymer/graphene oxide hydrogels for high-performance supercapacitors. *J Colloid Interface Sci*. 2019;560:69-76.
105. Li J, Zhang W, Zhang X, et al. Copolymer derived micro/meso porous carbon nanofibers with vacancy-type defects for high-performance supercapacitors. *J Mater Chem A*. 2019;8(5):2463-2471.
106. Fan L, Tu Q, Geng C, et al. High energy density and low self-discharge of a quasi-solid-state supercapacitor with carbon nanotubes incorporated redox-active ionic liquid-

based gel polymer electrolyte. *Electrochim Acta*. 2020;331:135425.
107. Zhang H, Li A, Yuan Y, et al. Preparation and characterization of colorful graphene oxide papers and flexible N-doping graphene papers for supercapacitor and capacitive deionization. *Carbon Energy*. 2020;2(4):656-674.
108. Yang ZC, Tang CH, Zhang Y, Gong H, Li X, Wang J. Cobalt monoxide-doped porous graphitic carbon microspheres for supercapacitor application. *Sci Rep*. 2013;3:2925.
109. Wang K, Zhang Z, Sun Q, Wang P, Li Y. Durian shell-derived N, O, P-doped activated porous carbon materials and their electrochemical performance in supercapacitor. *J Mater Sci*. 2020;55(1):10142-10154.
110. Subramani K, Shunmugasundaram S, Duraisamy V, Ilavarasi R, Kumar SMS, Sathish M. Dual heteroatoms doped SBA-15 templated porous carbon for symmetric supercapacitor in dual redox additive electrolyte. *J Colloid Interface Sci*. 2021;606(20):286-297.
111. John AR, Arumugam P. Open ended nitrogen-doped carbon nanotubes for the electrochemical storage of energy in a supercapacitor electrode. *J Power Sources*. 2015;277(1):387-392.
112. Kim JH, Ko Y, Kim YA, Kim KS, Yang CM. Sulfur-doped carbon nanotubes as a conducting agent in supercapacitor electrodes. *J Alloys Compd*. 2021;855:157282.
113. Yu X, Pei C, Feng L. Surface modulated hierarchical graphene film via sulfur and phosphorus dual-doping for high performance flexible supercapacitors. *Chin Chem Lett*. 2019;30(5):1121-1125.
114. Zhang JL, Xing LB, Liu TZ, et al. Three-dimensional reduced graphene hydrogels using various carbohydrates for high performance supercapacitors. *J Nanosci Nanotechnol*. 2017;17(2):1099-1107.
115. Miao L, Duan H, Zhu D, et al. Boron "gluing" nitrogen heteroatoms in a prepolymerized ionic liquid-based carbon scaffold for durable supercapacitive activity. *J Mater Chem A*. 2021;9(5):2714-2724.
116. Wang L, Liu H, Zhao J, et al. Enhancement of charge transport in porous carbon nanofiber networks via ZIF-8-enabled welding for flexible supercapacitors. *Chem Eng J*. 2019;382:122979.
117. Du J, Zhang Y, Wu H, Hou S, Chen A. N-doped hollow mesoporous carbon spheres by improved dissolution-capture for supercapacitors. *Carbon*. 2020;156:523-528.
118. Song Z, Duan H, Miao L, et al. Carbon hydrangeas with typical ionic liquid matched pores for advanced supercapacitors. *Carbon*. 2020;168:499-507.
119. Chee WK, Lim HN, Zainal Z, et al. Electrospun graphene nanoplatelets-reinforced carbon nanofibers as potential supercapacitor electrode. *Mater Lett*. 2017;199:200-203.
120. Ghanashyam G, Jeong HK. A thermally reduced graphite oxide and carbon nanotube composite for supercapacitor applications. *New Phys Sae Mulli*. 2018;68(2):181-184.
121. Zhou Y, Hu X, Guo S, Yu C, Zhang S, Liu X. Multi-functional graphene/carbon nanotube aerogels for its applications in supercapacitor and direct methanol fuel cell. *Electrochim Acta*. 2018;264:12-19.
122. Wang ZH, Yang JY, Wu XW, Chen XQ, Yu JG, Wu YP. Enhanced electrochemical performance of porous activated carbon by forming composite with graphene as high-performance supercapacitor electrode material. *J Nanopart Res*. 2017;19(2):1-10.
123. Niu Z, Zhang Y, Zhang Y, Lu X, Liu J. Enhanced electrochemical performance of three-dimensional graphene/carbon nanotube composite for supercapacitor application. *J Alloys Compd*. 2019;820:153114.
124. Adusei PK, Kanakaraj SN, Gbordzoe S, et al. A scalable nano-engineering method to synthesize 3D-graphene-carbon nanotube hybrid fibers for supercapacitor applications. *Electrochim Acta*. 2019;312:411-423.
125. Ye J, Hu B, Jin Y, et al. Interface engineering integrates fractal-tree structured nitrogen-doped graphene/carbon nanotubes for supercapacitors. *Electrochim Acta*. 2020;349:136372.
126. Liu K, Yao Y, Lv T, et al. Textile-like electrodes of seamless graphene/nanotubes for wearable and stretchable supercapacitors. *J Power Sources*. 2020;446:227355.
127. Lin XQ, Wang WD, Lü QF, Jin YQ, Lin Q, Liu R. Nitrogen-doped graphene/carbon nanohorns composite as a high-performance supercapacitor electrode. *J Mater Sci Technol*. 2017;33(11):1339-1345.
128. Liu T, Zhang X, Liu K, et al. A novel and facile synthesis approach of porous carbon/graphene composite for the supercapacitor with high performance. *Nanotechnology*. 2018;29(9):095401.
129. Li Q, Hu M, Wang K, Wang X. One-step approach for fabrication of 3D porous carbon/graphene composites as supercapacitor electrode materials. *Catal Today*. 2019;330:228-239.
130. Yang Q, Yang J, Gao Z, Li B, Xiong C. Carbonized cellulose nanofibril/graphene oxide composite aerogels for high-performance supercapacitors. *ACS Appl Energy Mater*. 2020;3(1):1145-1151.
131. Wan L, Shamsaei E, Easton CD, et al. ZIF-8 derived nitrogen-doped porous carbon/carbon nanotube composite for high-performance supercapacitor. *Carbon*. 2017;121:330-336.
132. Fu X, Chen A, Yu Y, Hou S, Liu L. Carbon nanotube@N-doped mesoporous carbon composite material for supercapacitor electrode. *Chem Asian J*. 2019;14(5):634-639.
133. Kang C, Ko Y, Fujisawa K, et al. Hybridized double-walled carbon nanotubes and activated carbon as free-standing electrode for flexible supercapacitor applications. *Carbon Lett*. 2020;30(109):527-534.
134. Zhang Y, Zhen Z, Zhang Z, et al. In-situ synthesis of carbon nanotube/graphene composite sponge and its application as compressible supercapacitor electrode. *Electrochim Acta*. 2015;157:134-141.
135. Sengottaiyan C, Jayavel R, Shrestha RG, et al. Indium oxide/carbon nanotube/reduced graphene oxide ternary nanocomposite with enhanced electrochemical supercapacitance. *Bull Chem Soc Jpn*. 2019;92(3):521-528.

136. Xie S, Dong F, Li J. Flexible solid-state supercapacitor based on carbon nanotube/Fe_3O_4/reduced graphene oxide binary films. *ChemistrySelect*. 2019;4(1):437-440.
137. Maity CK, Hatui G, Sahoo S, Saren P, Nayak GC. Boron nitride based ternary nanocomposites with different carbonaceous materials decorated by polyaniline for supercapacitor application. *ChemistrySelect*. 2019;4(13):3672-3680.
138. Bonakdar M, Hosseini SR, Ghasemi S. Poly(o-Anisidine)/carbon nanotubes/graphene nanocomposite as a novel and cost-effective supercapacitor material. *Mater Sci Eng B*. 2021;267(2):115099.
139. Zhang ZJ, Song QZ, He WX, et al. Dual surface modification of carbon materials by polydopamine and phosphomolybdic acid for supercapacitor application. *Dalton Trans*. 2020;48(46):17321-17330.
140. Zhao P, Wang N, Yao M, Ren H, Hu W. Hydrothermal electrodeposition incorporated with CVD-polymerisation to tune PPy@MnO_2 interlinked core-shell nanowires on carbon fabric for flexible solid-state asymmetric supercapacitors. *Chem Eng J*. 2020;380:122488.
141. Liu Y, Xin N, Yang Q, Shi W. 3D CNTs/graphene network conductive substrate supported MOFs-derived CoZnNiS nanosheet arrays for ultra-high volumetric/gravimetric energy density hybrid supercapacitor. *J Colloid Interface Sci*. 2021;583:288-298.
142. Gorduk O, Gencten M, Gorduk S, Sahin M, Sahin Y. Electrochemical fabrication and supercapacitor performances of metallo phthalocyanine/functionalized-multiwalled carbon nanotube/polyaniline modified hybrid electrode materials. *J Energy Storage*. 2020;33:102049.
143. Patil AM, An X, Li S, et al. Fabrication of three-dimensionally heterostructured rGO/WO_3·0.5H_2O@Cu_2S electrodes for high-energy solid-state pouch-type asymmetric supercapacitor. *Chem Eng J*. 2021;403:126411.
144. Kshetri T, Tran DT, Nguyen DC, Kim NH, Lau K, Lee JH. Ternary graphene-carbon nanofibers-carbon nanotubes structure for hybrid supercapacitor. *Chem Eng J*. 2020;380:122543.
145. Hekmat F, Hosseini H, Shahrokhian S, Emrah UH. Hybrid energy storage device from binder-free zinc-cobalt sulfide decorated biomass-derived carbon microspheres and pyrolyzed polyaniline nanotube-iron oxide. *Energy Storage Mater*. 2020;25:621-635.
146. Dang T, Wei D, Zhang G, et al. Homologous NiCoP/CoP heteronanosheets supported on N-doped carbon nanotubes for high-rate hybrid supercapacitors. *Electrochim Acta*. 2020;341:135988.
147. Mei L, Cui X, Duan Q, Li Y, Lv X, Wang H. Metal phthalocyanine-linked conjugated microporous polymer hybridized with carbon nanotubes as a high-performance flexible electrode for supercapacitors. *Int J Hydrogen Energy*. 2020;45(43):22950-22958.
148. Huang J, Song X, He C, Zhang Z, Qu L, Zhao D. Preparation and performance of multiwall carbon nanotubes/$FeNi_3$/polyaniline composite electrode material for supercapacitors. *Ionics*. 2020;26(5):2525-2536.
149. Zhang H, Wang B, Brown B. Atomic layer deposition of titanium oxide and nitride on vertically aligned carbon nanotubes for energy dense 3D microsupercapacitors. *Appl Surf Sci*. 2020;521:146349.
150. Wang L, Wen L, Tong Y, et al. Photo-rechargeable batteries and supercapacitors:Critical roles of carbon-based functional materials. *Carbon Energy*. 2021;3(2):225-252.
151. Li Y, Yang Y, Zhou J, et al. Coupled and decoupled hierarchical carbon nanomaterials toward high-energy-density quasi-solid-state Na-Ion hybrid energy storage devices. *Energy Storage Mater*. 2019;23:530-538.
152. Wei G, Zhao X, Du K, et al. A general approach to 3D porous CQDs/M_xO_y (M=Co, Ni) for remarkable performance hybrid supercapacitors. *Chem Eng J*. 2017;326:58-67.
153. Hu M, Cui C, Shi C, et al. High-energy-density hydrogen-ion-rocking-chair hybrid supercapacitors based on $Ti_3C_2T_x$ MXene and carbon nanotubes mediated by redox active molecule. *ACS Nano*. 2019;13(6):6899-6905.
154. Liu K, Yu C, Guo W, et al. Recent research advances of self-discharge in supercapacitors: mechanisms and suppressing strategies. *J Energy Chem*. 2021;16(7):94-109.
155. Zhang Q, Cai C, Qin J, Wei B. Tunable self-discharge process of carbon nanotube based supercapacitors. *Nano Energy*. 2014;4:14-22.
156. Du Y, Mo Y, Chen Y. Effects of Fe impurities on self-discharge performance of carbon-based supercapacitors. *Materials*. 2021;14(8):1908.
157. Li Y, Yang W, Yang W, et al. Towards high-energy and anti-self-discharge Zn-ion hybrid supercapacitors with new understanding of the electrochemistry. *Nano-Micro Lett*. 2021;13(1):95.
158. Su X, Jia W, Ji H, Zhu Y. Mitigating self-discharge of activated carbon-based supercapacitors with hybrid liquid crystal as an electrolyte additive. *J Energy Storage*. 2021;41:102830.
159. Wang K, Yao L, Jahon M, et al. Ion-exchange separators suppressing self-discharge in polymeric supercapacitors. *ACS Energy Lett*. 2020;5(10):3276-3284.

AUTHOR BIOGRAPHIES



Mingzhu Zhong is a student at the School of Physics and Materials Science, Tianjin Normal University, China, under the supervision of Dr. Miao Zhang. Her research focuses on the carbon nanomaterials for supercapacitors.



Miao Zhang is a research associate at the School of Physics and Materials Science, Tianjin Normal University, China. She received her PhD degree from Tianjin University in 2017. Her current research interest mainly focuses

on energy storage, such as lithium-ion batteries and supercapacitors.



Xifei Li is a professor and doctoral supervisor at Xi'an University of Technology, China. He is the executive editor of Springer nature's Sci academic journal electrochemical energy reviews (impact factor has exceeded 27), vice chairman of the fuel cell engine branch of China's internal combustion engine society, and so forth, mainly engaged in the design and optimization of micro/nano functional material interface and the application research of secondary battery.

How to cite this article: Zhong M, Zhang M, Li X. Carbon nanomaterials and their composites for supercapacitors. *Carbon Energy*. 2022;4:950-985. doi:10.1002/cey2.219